Computation of sharp estimates of the Poincaré constant on planar domains with piecewise self-similar boundary

Lehel Banjai and Lyonell Boulton

Abstract. We establish a strategy for finding sharp upper and lower numerical bounds of the Poincaré constant on a class of planar domains with piecewise self-similar boundary. The approach consists of four main components: W1) tight inner-outer shape interpolation, W2) conformal mapping of the approximate polygonal regions, W3) grad-div system formulation of the spectral problem and W4) computation of the eigenvalue bounds. After describing the method, justifying its validity and determining general convergence estimates, we show concrete evidence of its effectiveness by computing lower and upper bound estimates for the constant on the Koch snowflake.

Contents

1. Introduction

The Poincaré constant $\kappa_g > 0$ of a planar open set Σ is the smallest $\kappa > 0$ for which

$$\int_\Sigma |u|^2 \leq \kappa \int_\Sigma |\operatorname{grad} u|^2 \quad \text{for all } u \in H_0^1(\Sigma).$$

Namely, $\omega_1^2 = \frac{1}{\kappa_g}$ is the ground eigenvalue of the Dirichlet Laplacian on Σ. When the boundary $\partial\Sigma$ is a fractal curve, finding accurate estimates for this constant is highly non-trivial. Classically, much of the important work in this area [23, 30] has focused on determining asymptotics for ω_1^2 in terms of inner approximations of Σ, with the notable exception of a few numerical results reported in the literature for the particular case of the Koch snowflake [22, 19, 28, 1].

In this paper we describe a method for computing tight upper and lower approximations of κ_g, when there exist two sequences of simply connected open polygons, $\{T_j\}_{j=0}^\infty$ and $\{H_j\}_{j=0}^\infty$, such that

$$T_j \subset T_{j+1} \subset \Sigma \subset H_{j+1} \subset H_j \quad \text{for all } j \geq 0 \qquad (A1)$$

and for all $\varepsilon > 0$ there exists $k \in \mathbb{N}$ such that[1]

$$\{z \in H_j : \operatorname{dist}(z, \partial H_j) \geq \varepsilon\} \subset T_j \quad \text{for all } j \geq k. \qquad (A2)$$

This implies that

$$\Sigma = \bigcup_{j=0}^\infty T_j = \operatorname{int}\left(\bigcap_{j=0}^\infty H_j\right).$$

Our main interest is for the boundary, $\partial\Sigma$, to be a fractal curve. The strategy that we present next combines the use of conformal mappings [1, 3] and a grad-div system formulation of the problem, with the quadratic projection method [24, 32, 14].

Workflow of the method (upper and lower bounds for κ_g). We proceed in four steps.

W1) *Embedding of the region and domain monotonicity.* Find polygons satisfying (A1). By domain monotonicity, upper (and lower) bounds for the Poincaré constant in H_j (and T_j) give upper (and lower) bounds for κ_g. Below Ω_j denotes either H_j or T_j.

---

[1] Here and elsewhere below we simplify the notation as follows, $\operatorname{dist}(x, A) = \inf\{|x - a| : a \in A\}$ for a point x and a set A, but $\operatorname{dist}(A, B)$ will be the Hausdorff distance between two sets A and B.

W2) *Conformal transplantation.* Determine conformal maps $\Omega_0 \to \Omega_j$. The eigenvalue problem on Ω_j is transformed into a pencil eigenvalue problem on Ω_0 with a singular j-dependent right hand side.

W3) *Formulation as a system.* For fixed j, write the pencil eigenvalue problem on Ω_0 as a first order system involving the gradient operator, the divergence operator and singular coefficients.

W4) *Computation of the upper and lower bounds.* Compute enclosures for the smallest positive eigenvalues of the singular first order systems by means of a pollution-free projection method. To make this concrete we choose the quadratic projection method.

Below we often refer to the fixed j in any of the blocks W1)-W4), by saying that the relevant datum is associated to the level j.

In this scheme, our precise hypotheses on Σ and $\partial\Sigma$ are as follows.

Assumption A. The region $\Sigma \subset \mathbb{R}^2$ is open and simply connected. There exist two sequences of simply connected polygons satisfying (A1) and (A2). Additionally,

(A3) the boundary is given by

$$\partial\Sigma = \bigcup_{n=1}^{N} F_n$$

where F_n are self-similar curves each associated to an iterated function scheme,

(A4) the vertices of ∂T_j and ∂H_j are computable from these iterated function schemes.

As written in the Assumption A, (A4) is not mathematically concrete and its proper formulation for particular cases is clarified in Section 2. If Σ is a Koch snowflake, for example, T_j can be chosen to be the classical jth step of the construction starting from T_0 an equilateral triangle. And H_j the less standard but well known jth step of the construction starting from a hexagon H_0, see [25, Plate 37], [26, Plate 43] and Figure 1 below. Hence, in this case (A4) is guaranteed by construction.

In Section 2 we describe and justify the block W1) in the workflow given this hypothesis. In particular the Assumption A covers classical domains with fractal boundary, but in the construction of T_j and H_j, both (A1) and (A2) demand careful attention. We determine this specific construction for: a Koch snowflake, a Cèsaro

(generalised Koch) snowflake of any angle [10], a quadric island [25, Plate 49] and a Gosper–Peano island [25, Plate 47], [17]. In lemmas 2.1, 2.2, and 2.6, we establish convergence of the eigenvalue bounds of block W1) as $j \to \infty$, by applying directly an estimate of Pang [30].

The singularities of the derivative of the conformal maps associated to block W2) determine the domain of the grad-div matrix operator in the formulation of block W3). In Section 3 we conduct a detailed analysis of these singularities. In Section 4, on the other hand, we describe the precise operator-theoretical setting of the grad-div singular eigenvalue problem. Several technical details in this respect are given in the Appendix A.

The reduction to a grad-div formulation proposed in block W3) is not standard in the context of eigenvalue computation for the Laplacian. It is also counter-intuitive, as one is left with an indefinite eigenvalue problem which is prone to spectral pollution due to variational collapse. However, an order reduction of the differential operator often improves the accuracy of a non-pollution projection method [5, 6, 4]. We have chosen the quadratic method. In Section 5 we survey this method and establish the details of its justification.

Section 6 is devoted to a full concrete implementation of W1)-W4) for Σ a Koch snowflake inscribed in the unit circle. We report on details of our calculations leading towards the following estimate

$$13.1160115 \leq \frac{1}{\kappa_{\mathrm{g}}} \leq 13.1162276. \tag{1}$$

See Table 1. Remarkably, by formulation of the method, neither the computation nor the validation of these bounds relies on asymptotic arguments.

2. Embedding of the region and domain monotonicity

Consider the eigenvalue problem associated with the Dirichlet Laplacian,

$$\begin{aligned} -\Delta u &= \omega^2 u \quad \text{in } \Omega, \\ u &= 0 \qquad \text{on } \partial\Omega, \end{aligned} \tag{2}$$

on a simply connected open set Ω. By virtue of the classical min-max principle, $\kappa_{\mathrm{g}} = \frac{1}{\omega_1^2}$ where $\omega_1 \equiv \omega_1(\Sigma) > 0$ is the square root of the first eigenvalue of (2) for $\Omega = \Sigma$. Domain monotonicity ensures that

$$\Omega \subset \tilde{\Omega} \implies \omega_k^2(\tilde{\Omega}) \leq \omega_k^2(\Omega). \tag{3}$$

We will, in particular, repeatedly use this property for $k = 1$ and $k = 2$.

Combining the embedding condition (A1) with (3) yields

$$\omega_1^2(\mathsf{H}_j) \leq \omega_1^2(\Sigma) \leq \omega_1^2(\mathsf{T}_j).$$

The next lemma is crucial to our analysis. Its proof is an immediate consequence of a uniform estimate on $\omega_j^2(\Omega)$ from inner approximations of Ω established by Pang [30, Theorem 1.1]. Here and elsewhere $j_{0,1} \approx 5.784$ is the first eigenvalue of (2) for Ω the unit disk.

Lemma 2.1. *Let $\{\mathsf{T}_j\}_{j=0}^{\infty}$ and $\{\mathsf{H}_j\}_{j=0}^{\infty}$ be two families of open simply connected polygons, such that $\mathsf{T}_j \subset \mathsf{T}_{j+1} \subset \mathsf{H}_{j+1} \subset \mathsf{H}_j$ and such that (A2) holds true. Let*

$$C = \frac{2^9 j_{0,1}^4 S^{9/4}}{3\pi^{9/4} R^7}$$

where $S = |\mathsf{H}_0|$ and R is the inradius of T_0,

$$R = \sup_{z \in \mathsf{T}_0} \mathrm{dist}(z, \partial \mathsf{T}_0).$$

For $\varepsilon > 0$, the same $k \in \mathbb{N}$ satisfying (A2) yields

$$\omega_1^2(\mathsf{T}_j) - \omega_1^2(\mathsf{H}_j) \leq C\varepsilon^{1/2} \quad \text{for all } j \geq k.$$

Proof. Apply directly [30, Theorem 1.1], observing that $|\mathsf{H}_0| \geq |\mathsf{H}_j|$ and that the inradius of T_0 is less than or equal the inradiuses of H_j. □

Thus (A1) and (A2) imply that, in the context of the block W1),

$$\omega_1^2(\mathsf{T}_j) \longrightarrow \omega_1^2(\Sigma) \quad \text{and} \quad \omega_1^2(\mathsf{H}_j) \longrightarrow \omega_1^2(\Sigma), \quad \text{for } j \to \infty, \qquad (4)$$

monotonically. Note that weaker versions of this result can also be established if T_j or H_j are not nested.

2.1. The classical Koch snowflake. We first describe a specific construction of T_j and H_j for a Koch snowflake. Scale Σ such that it is inscribed in a unit circle. Let T_0 be an equilateral triangle of side length $\sqrt{3}$ and H_0 a hexagon of side length 1, both centred at 0, such that T_0 is inscribed in H_0. The polygon T_j is constructed by attaching to the central third of each side of T_{j-1} an equilateral triangle, whereas the polygon H_j is constructed from H_{j-1} by subtracting an equilateral triangle. The two procedures have the following generators, with T_j at the top and H_j at the bottom:
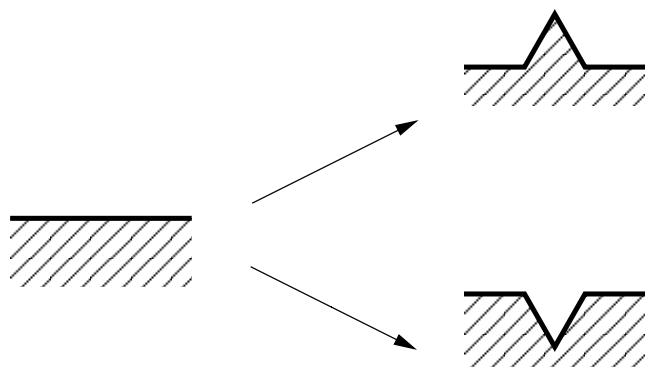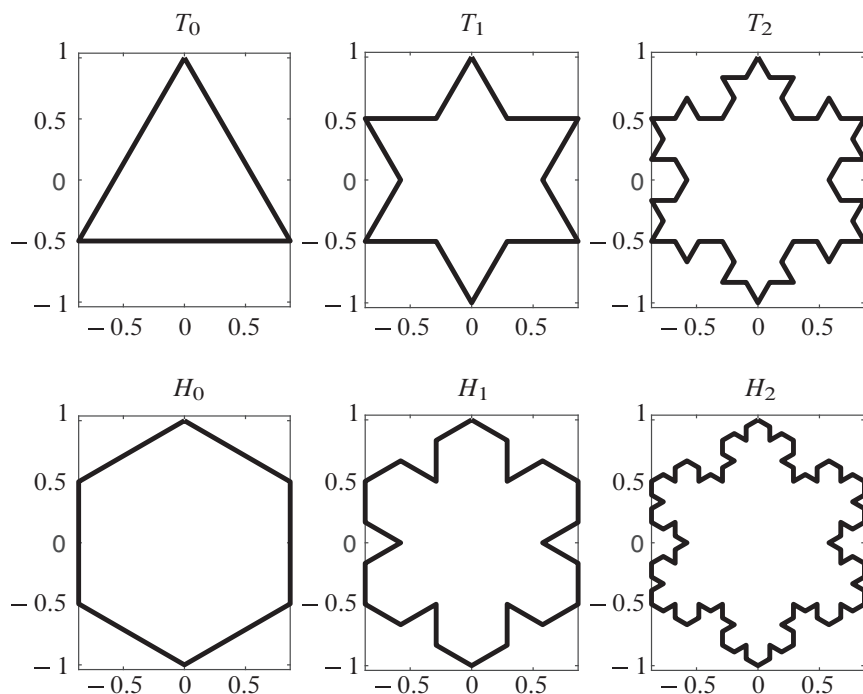
The resulting polygons for levels $j = 0, 1, 2$ are shown in Figure 1.

Figure 1. Three levels of T_j and H_j for the Koch snowflake.

Lemma 2.2. *Let T_j and H_j be as described in the preceding paragraph. Then,* $\mathsf{T}_j \subset \mathsf{T}_{j+1} \subset \mathsf{H}_{j+1} \subset \mathsf{H}_j$ *for all* $j \geq 0$ *and* (A2) *holds true. Moreover*

$$\omega_1^2(\mathsf{T}_j) - \omega_1^2(\mathsf{H}_j) \leq \frac{j_{0,1}^4 3^{3/4}}{2^{5/4}\pi^{9/4}}\left(\frac{1}{\sqrt{3}}\right)^j \quad \text{for all } j \in \mathbb{N}. \tag{5}$$

Proof. We claim that polygon H_j is obtained by attaching to each edge of T_j an isosceles triangle whose base is this edge and whose height is $\frac{1}{2\sqrt{3}}$ times the length of the edge. From this, it follows that $\mathsf{T}_j \subset \mathsf{H}_j$ and that

$$\left\{ z \in \mathsf{H}_j : \operatorname{dist}(z, \partial \mathsf{H}_j) \geq \frac{1}{3^{j+1}} \right\} \subset \mathsf{T}_j.$$

The latter implies (A2). Then, (5) follows from Lemma 2.1, taking $\varepsilon = \frac{1}{3^{j+1}}$ and $R = 1$.

It remains to prove the claim by induction. It is not difficult to check that the claim holds for $j = 0$. Next, assume that it holds for some $j = k \geq 0$. After rotation and translation let AB with $A = (0,0)$, $B = (\ell, 0)$ and $\ell = 3^{-k}\sqrt{3}$ be an edge of T_k; see Figure 2. Then by assumption BC and CA are edges of H_k where $C = \left(\frac{\ell}{2}, \frac{\ell}{2\sqrt{3}}\right)$. By the definition of polygons T_j, AD and DC are edges of T_{k+1} where $D = \left(\frac{\ell}{3}, 0\right)$. Further, by the definition of polygons H_j, AE, ED, DF and FC are edges of H_{k+1} where $E = \left(\frac{\ell}{6}, \frac{\ell}{6\sqrt{3}}\right)$ and $F = \left(\frac{\ell}{3}, \frac{\ell}{3\sqrt{3}}\right)$. As triangles ADE and DCF are of the required shape, we have proved the claim for $j = k+1$ and hence by induction for all $j \geq 0$. $\qquad\square$
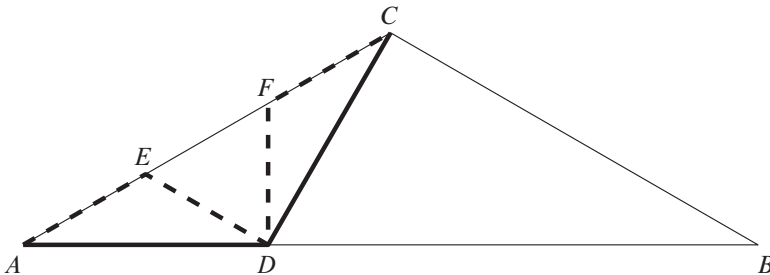

Figure 2. A diagram in aid of Lemma 2.2 explaining the connection between T_j and H_j.

Let

$$\Omega_{\mathsf{T}} = \bigcup_{j=0}^{\infty} \mathsf{T}_j \quad \text{and} \quad \Omega_{\mathsf{H}} = \operatorname{int}\left(\bigcap_{j=0}^{\infty} \mathsf{H}_j \right).$$

As a consequence of the previous lemma $\Omega_{\mathsf{T}} = \Omega_{\mathsf{H}}$. When referring to the Koch snowflake below, without further mention, we are setting $\Sigma = \Omega_{\mathsf{T}} = \Omega_{\mathsf{H}}$. In this case, (A1) and (A2) hold true, the condition (A3) is given by F_1, F_2 and F_3, which are Koch curves, and (A4) is intrinsic to the construction.

Remark 2.3. In the proof of Lemma 2.1 we have employed the general estimate of Pang, which applies to a large class of regions. As it is natural to expect and as

we shall see from numerical evidence presented in Section 6, the rate factor $\frac{1}{\sqrt{3}}$ in (5) is sub-optimal for the specific approximation of the Koch snowflake by T_j and H_j. Our evidence suggests that

$$\omega_1^2(\mathsf{T}_j) - \omega_1^2(\mathsf{H}_j) \approx C\varrho^j \quad \text{where } \varrho \approx 0.35958, \ C \approx 5.8688.$$

See Table 2.

2.2. General Koch curves. The sequences $\{\mathsf{T}_j\}$ and $\{\mathsf{H}_j\}$ can be constructed in similar way as above, if $\partial\Sigma$ is the union of several boundary components F_n in (A3), all of them being Koch curves with a generator of the following form.
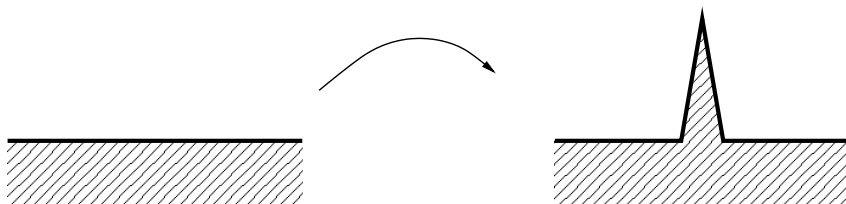
In the L-system language [31], F_n has generator `"F"->"F+F--F+F"` with the same angle $0 < \alpha < \pi/2$. In particular, let T_0 be a regular N-gon. The polygon T_j is obtained by attaching to the center of each side of T_{j-1} an isosceles triangle whose sides are equal to the length of the other two sides remaining in the segment. Polygons H_j are then constructed from these polygons T_j in a similar way as in the proof of Lemma 2.2. Namely, H_j is obtained by attaching to each edge of T_j an isosceles triangle whose base is this edge and whose height is $\left(\tan\frac{\alpha}{2}\right)$ times the length of the edge.

A similar approach also works for antisnowflakes. For example F_n could be Cèsaro curves [10] of the form `"F"->"F-F++F-F"` of any angle swapping the way the polygons T_j and H_j are constructed.

In both these constructions, the validity of the Assumption A is ensured by a statement very similar to Lemma 2.2 with a proof which is almost identical. We omit further details.

2.3. Other fractal curves with simple generators. We now establish a principle for constructing inner-outer polygonal approximations satisfying the Assumption A, which apply to other classes of regions with piecewise self-similar boundary. As we shall see later, this includes classical fractals such as those shown in Figure 3. We begin by developing a necessary notation and formulating a general result about simply connected polygons.
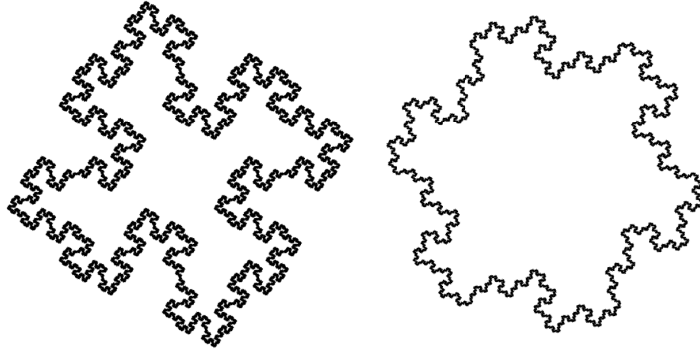
Figure 3. Quadric island (left) and Gosper–Peano island (right).

The open ε-neighbourhood in Euclidean distance of a set $\mathsf{S} \subset \mathbb{R}^2$ will be written as $(\mathsf{S})_\varepsilon$. Let $\mathsf{S} \subset \mathbb{R}^2$ be an open bounded polygon such that $\partial\mathsf{S}$ is a closed Jordan curve. Order the segments on the boundary of S, σ_k, contiguously: such that

$$\partial\mathsf{S} = \bigcup_{k=1}^{M} \sigma_k$$

and $\sigma_j \cup \sigma_{j+1}$ is a continuous curve for all $j = 1, \dots, M$ denoting $\sigma_{M+1} = \sigma_1$.

Let $\mathbb{V}(\mathsf{S})$ be the set of vertices/corners on $\partial\mathsf{S}$. Let $\varepsilon > 0$. Let $A \in \mathbb{V}(\mathsf{S})$ be a corner point of inner angle $\beta \equiv \beta(A)$. Denote by $A_\varepsilon^{\mathrm{i}}$ the unique point on the segment bisecting $\beta(A)$ at distance $\frac{\varepsilon}{\sin\frac{\beta}{2}}$ from A. Denote by $A_\varepsilon^{\mathrm{o}}$ the unique point on the segment bisecting the complementary angle to $\beta(A)$ at distance $\frac{\varepsilon}{\sin\frac{\beta}{2}}$ from A. That is $A_\varepsilon^{\mathrm{i}}$ and $A_\varepsilon^{\mathrm{o}}$ are endpoints of a line segment that also passes through A. Because $\partial\mathsf{S}$ is a closed Jordan curve which is piecewise linear, and all angles $\beta(A) \in (0, 2\pi)$, there exists ε_0 such that $A_\varepsilon^{\mathrm{i}} \in \mathsf{S}$ and $A_\varepsilon^{\mathrm{o}} \notin \mathsf{S}$ for all $0 < \varepsilon < \varepsilon_0$ and $A \in \mathbb{V}(\mathsf{S})$. Indeed this is a consequence of the fact that the line segments $[A_\varepsilon^{\mathrm{i}}, A_\varepsilon^{\mathrm{o}}]$ have midpoint A and $A_\varepsilon^{\mathrm{i};\mathrm{o}} \to A$ as $\varepsilon \to 0$.

For the side $\sigma_j = [A, B]$, set $\mathsf{Q}_\varepsilon^j \equiv \mathsf{Q}_\varepsilon^j(\mathsf{S})$ to be the open quadrilateral (trapezoid or rhomboid) with vertices $A_\varepsilon^{\mathrm{i}}$, $A_\varepsilon^{\mathrm{o}}$, $B_\varepsilon^{\mathrm{i}}$, $B_\varepsilon^{\mathrm{o}}$. That is two sides of Q_ε^j are parallel to σ_j at distance ε from this segment, another is $[A_\varepsilon^{\mathrm{i}}, A_\varepsilon^{\mathrm{o}}]$ and the other is $[B_\varepsilon^{\mathrm{i}}, B_\varepsilon^{\mathrm{o}}]$. For $0 < \varepsilon < \varepsilon_0$, we will write

$$[\mathsf{S}]_\varepsilon^{\mathrm{i}} = \mathsf{S} \setminus \left(\bigcup_{j=1}^{M} \overline{\mathsf{Q}_\varepsilon^j} \right) \quad \text{and} \quad [\mathsf{S}]_\varepsilon^{\mathrm{o}} = \mathsf{S} \cup \mathrm{int}\left(\bigcup_{j=1}^{M} \overline{\mathsf{Q}_\varepsilon^j} \right).$$

Then

$$[\mathsf{S}]_\varepsilon^\mathrm{i} \subset \mathsf{S} \subset [\mathsf{S}]_\varepsilon^\mathrm{o} \qquad \text{and} \qquad (\partial \mathsf{S})_\varepsilon \subset \bigcup_{k=1}^M \overline{\mathsf{Q}_\varepsilon^k} = \overline{[\mathsf{S}]_\varepsilon^\mathrm{o}} \setminus [\mathsf{S}]_\varepsilon^\mathrm{i}.$$

Let

$$\beta_\mathrm{m}(\mathsf{S}) = \max_{A \in \mathbb{V}(\mathsf{S})} \{\beta(A), 2\pi - \beta(A)\} \in (\pi, 2\pi)$$

be the maximal angle among all angles (inner and outer) in $\partial \mathsf{S}$. Since

$$\mathrm{dist}\left(y, \partial \bigcup_{k=1}^M \overline{\mathsf{Q}_\varepsilon^k}\right) \le \frac{\varepsilon}{\sin \frac{\beta_\mathrm{m}(\mathsf{S})}{2}} \qquad \text{for all } y \in \partial \mathsf{S},$$

then

$$[\mathsf{S}]_\varepsilon^\mathrm{o} \setminus \overline{[\mathsf{S}]_\varepsilon^\mathrm{i}} \subset (\partial \mathsf{S})_{\tilde\varepsilon} \quad \text{for } \tilde\varepsilon = \frac{\varepsilon}{\sin \frac{\beta_\mathrm{m}(\mathsf{S})}{2}}. \tag{6}$$

The proof of the following lemma is a straightforward consequence of the fact that $\mathrm{dist}(\overline{[\mathsf{S}]_\varepsilon^\mathrm{o} \setminus [\mathsf{S}]_\varepsilon^\mathrm{i}}, \partial \mathsf{S}) \to 0$ as $\varepsilon \to 0$.

Lemma 2.4. *There exists $\varepsilon_1 > 0$ such that the following holds true for all $0 < \varepsilon < \varepsilon_1$. The intersection $\mathsf{Q}_\varepsilon^m \cap \mathsf{Q}_\varepsilon^n = \varnothing$ for $m \ne n$ and the sets $[\mathsf{S}]_\varepsilon^\mathrm{i}$ and $[\mathsf{S}]_\varepsilon^\mathrm{o}$ are simply connected.*

We now determine concrete sufficient conditions for a region Σ to satisfy the Assumption A.

Hypothesis G. Let Σ be an open planar region such that $\partial \Sigma = \bigcup_{n=1}^N F_n$ is a Jordan curve and F_n are self-similar curves. Let Σ_j be the resulting open pre-fractal polygons. That is, $\partial \Sigma_j$ is the union of the steps j in the generation of the F_n for $n = 1, \ldots, N$. Suppose that all $\partial \Sigma_j$ are Jordan curves, that there is $\beta_0 \in (\pi, 2\pi)$ such that $\beta_\mathrm{m}(\Sigma_j) \le \beta_0$ and that all the polygons Σ_j have all their sides of equal length, ℓ_j, where $\ell_j > \ell_{j+1} \to 0$. Additionally write $\mathsf{Q}_\varepsilon^{m,j} = \mathsf{Q}_\varepsilon^m(\Sigma_j)$. Suppose that there exists a constant $\delta > 0$ such that for all $j \in \mathbb{N}$

(G1) $\mathsf{Q}_{\delta\ell_j}^{m,j} \cap \mathsf{Q}_{\delta\ell_j}^{n,j} = \varnothing$ for $m \ne n$,

(G2) the sets

$$\mathsf{T}_j = [\Sigma_j]_{\delta\ell_j}^\mathrm{i} \quad \text{and} \quad \mathsf{H}_j = [\Sigma_j]_{\delta\ell_j}^\mathrm{o}$$

are simply connected,

(G3) $(\mathsf{H}_{j+1} \setminus \mathsf{T}_{j+1}) \subset (\mathsf{H}_j \setminus \mathsf{T}_j)$, and

(G4) $\bigcap_j \mathsf{T}_j \ne \varnothing$.

Lemma 2.5. *If the planar region* Σ *satisfies the Hypothesis G, then it satisfies the Assumption A.*

Proof. Hypothesis G already contains (A3). The condition (G1) implies that the vertices of T_j and H_j are respectively the vertices of $\mathsf{Q}^{m,j}_{\delta \ell_j}$ and we have an explicit formula for them in terms of the vertices of Σ_j. This is a concrete realisation of (A4).

Now, consider (A1). By construction we have that $\mathsf{T}_j \subset \Sigma_j \subset \mathsf{H}_j$. From (G2) it follows that $\mathbb{R}^2$ is split into three disjoint connected regions T_{j+1}, $\mathsf{H}_{j+1} \setminus \mathsf{T}_{j+1}$ and $\mathsf{H}^c_{j+1} = \mathbb{R}^2 \setminus \mathsf{H}_{j+1}$. From (G3) we have that $\mathsf{H}_j \cap (\mathsf{H}_{j+1} \setminus \mathsf{T}_{j+1}) = \varnothing$. Also $\mathsf{H}^c_{j+1} \not\subset \mathsf{T}_{j+1}$ because the left-hand side is unbounded. Hence, $\mathsf{H}^c_j \subset \mathsf{H}^c_{j+1}$ and so

$$\mathsf{H}_{j+1} \subset \mathsf{H}_j. \tag{7}$$

On the other hand (G3) also implies $\mathsf{T}_j \cap (\mathsf{H}_{j+1} \setminus \mathsf{T}_{j+1}) = \varnothing$, hence either $\mathsf{T}_j \subset \mathsf{T}_{j+1}$ or $\mathsf{T}_j \subset \mathsf{H}^c_{j+1}$. The latter contradicts (G4) and thus

$$\mathsf{T}_j \subset \mathsf{T}_{j+1}. \tag{8}$$

From (7) and (8) follows that

$$\mathsf{T}_j \subset \Sigma_{j+k} \subset \mathsf{H}_j \quad \text{for all } k \in \mathbb{N}. \tag{9}$$

Since the Hausdorff limit of a family of compact sets contains the intersection of this family and it is contained in the union of this family, (A1) is a consequence of (9).

We finally show (A2). Let $\varepsilon > 0$ and let $k > 0$ be such that

$$\ell_k < \frac{\varepsilon \sin \frac{\beta_0}{2}}{2\delta}.$$

For $j > k$, from the fact that ℓ_j are decreasing and in the notation of (6),

$$\widetilde{\delta \ell_j} = \frac{\delta \ell_j}{\sin \frac{\beta_{\mathrm{m}}(\Sigma_j)}{2}} < \frac{\delta \ell_k}{\sin \frac{\beta_0}{2}} < \frac{\varepsilon}{2}.$$

Then, from (6) it follows that

$$\mathrm{dist}(x, \partial[(\partial \Sigma_j)_{\widetilde{\delta \ell_j}}] \cap \Sigma_j) < 2\widetilde{\delta \ell_j} < \varepsilon \quad \text{for all } x \in \partial \mathsf{H}_j$$

and

$$\partial[(\partial \Sigma_j)_{\widetilde{\delta \ell_j}}] \cap \mathsf{T}_j = \partial[(\partial \Sigma_j)_{\widetilde{\delta \ell_j}}] \cap \Sigma_j = \partial[(\partial \Sigma_j)_{\widetilde{\delta \ell_j}}] \cap \mathsf{H}_j.$$

Hence, $\mathsf{H}_j \setminus (\partial \mathsf{H}_j)_\varepsilon \subset \mathsf{T}_j$. Thus (A2) holds true. $\qquad \square$

In the Hypothesis G, the conditions (G1) and (G2) contrast with (G3). That is, by Lemma 2.4, (G1) and (G2) are satisfied for δ small enough. They do not depend on the relation between different levels. But, as we shall see in the examples of the quadric and Gosper–Peano islands, (G3) will break for δ too close to 0. The condition (G4) is independent of any of this.

We now show a convergence estimate in the context of block W1) for the ground eigenvalues of T_j and H_j defined as in the Hypothesis G.

Lemma 2.6. *Let the planar region Σ satisfy the Hypothesis G. Let $C > 0$ be the constant of Lemma 2.1. Then*

$$\omega_1^2(\mathsf{T}_j) - \omega_1^2(\mathsf{H}_j) \leq \frac{C\sqrt{2\delta}}{\sin\left(\frac{\beta_0}{2}\right)^{\frac{1}{2}}} \ell_j^{\frac{1}{2}} \downarrow 0, \quad j \to \infty. \tag{10}$$

Proof. Under the conditions of the Hypothesis G,

$$\left\{ z \in \mathsf{H}_j : \operatorname{dist}(z, \partial\mathsf{H}_j) \geq \frac{2\delta\ell_j}{\sin\frac{\beta}{2}} \right\} \subset \mathsf{T}_j.$$

The conclusion follows by applying Lemma 2.1 and recalling that $\ell_j \to 0$ monotonically. $\square$

In this lemma, it is remarkable that the convergence rate of the eigenvalue gap is directly related to the decay rate of the ℓ_j. We now examine the Hypotheses G for two classical fractal region.

2.4. Quadric islands. Let Σ be a quadric island [25, Plate 49] constructed as follows. Begin with Σ_0 a square of side 1. Let F_n for $n = 1, \ldots, 4$ be constructed using the generator

See Figure 3 left.

Suppose that the sides of Σ_0 are aligned with the horizontal and vertical axes. Then, $\partial\Sigma_j$ is the union of two families, each comprising segments of equal length. One of these families is made of segments aligned with the horizontal axis and the other is made of segments aligned with the vertical axis. It is readily seen that

$$\ell_j = \frac{\ell_{j-1}}{4} = \frac{1}{4^j} \quad \text{and} \quad \beta_{\mathrm{m}}(\Sigma_j) = \frac{3\pi}{2}.$$

The trapezoids and rhomboids which jointly form $H_j \setminus \overline{T_j}$ always have two opposite edges parallel to the axes. Then, (G1) holds true for all $\delta \leq \frac{1}{2}$. Moreover, ∂T_j and ∂H_j are Jordan curves, so (G2) as well as (G4) are satisfied for all $\delta < \frac{1}{2}$.

On the other hand,

$$\text{dist}(\partial\Sigma_j, \partial\Sigma_{j+1}) = \ell_{j+1}.$$

Hence

$$\text{dist}(\partial\Sigma_j, \partial[(\Sigma_{j+1})_{\delta\ell_{j+1}}]) = (1 + \delta)\ell_{j+1}.$$

Thus, the condition (G3) holds if and only if

$$\delta\ell_j \geq (1 + \delta)\ell_{j+1}.$$

Solving for δ, we get that $\delta \geq \frac{1}{3}$. See Figure 4 (left).

This argumentation shows that for the quadric island with generator as above, the inner-outer interpolants T_j and H_j, as in the Hypothesis G, ensure the validity of the Assumption A for all $\frac{1}{3} \leq \delta < \frac{1}{2}$. Further, Lemma 2.6 implies that, for block W1), $\omega_1^2(T_j) - \omega_1^2(H_j) \to 0$ as $j \to \infty$ at a rate at least $\frac{1}{2^j}$.
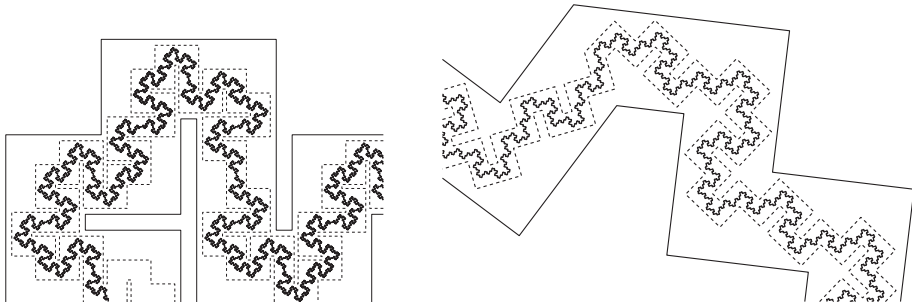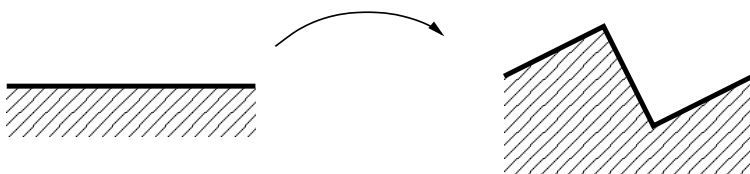

Figure 4. A section of the quadric island with T_j and H_j, for $j = 3, 4$ and $\delta = 0.4$ (left). A section of the Gosper–Peano island with T_j and H_j, for $j = 4, 6$ and $\delta = 0.48$ (right).

2.5. Gosper–Peano islands. As a final example, we consider Σ to be a Gosper–Peano island [25, Plate 47], in which Σ_0 is a hexagon of side 1. See Figure 3 right. That is F_n for $n = 1, \ldots, 6$ is constructed using the generator

The boundary $\partial\Sigma_j$ is a union of equal length segments where

$$\ell_j = \frac{\ell_{j-1}}{\sqrt{5}} = \frac{1}{5^{\frac{j}{2}}}.$$

As we will see next, there is no $\delta > 0$ ensuring all three conditions of the Hypothesis G simultaneously. After that, we show how to overcome this difficulty, which is not caused by the fact that Σ_0 is a hexagon.

The inner angles of the vertices in each of the 6 components of $\partial\Sigma_j$ are either $\beta = \frac{\pi}{2}$ or $\beta = \frac{3\pi}{2}$. Each one of these components is an arrangement of segments (of the same length) aligned in two possible directions one perpendicular to the other. The inner angle between components is a fixed $\beta = \frac{2\pi}{3}$. So $\beta_m(\Sigma_j) = \frac{3\pi}{2}$. Then, similar to the case of the quadric island, (G1), (G2), and (G4) are satisfied if and only if $0 < \delta < \frac{1}{2}$.

Now,

$$\mathrm{dist}(\partial\Sigma_j, \partial[(\Sigma_{j+1})_{\delta\ell_{j+1}}]) = \frac{\ell_j}{5} + \frac{\delta\ell_{j+1}}{\frac{\sqrt{2}}{2}}\sin\left(\alpha + \frac{\pi}{4}\right) = \frac{\ell_j}{5} + \delta\ell_j\frac{3}{5}$$

where $\alpha = \arcsin(1/\sqrt{5})$ is the angle between the j and $j+1$ iteration. In order to satisfy (G3), we require

$$\mathrm{dist}(\partial\Sigma_j, \partial[(\Sigma_{j+1})_{\delta\ell_{j+1}}]) < \delta\ell_j.$$

Solving for δ gives $\delta > \frac{1}{2}$. So indeed, there is no $\delta > 0$ such that (G3) holds at the same time as (G1), (G2), and (G4).

To construct an approximating sequence of inner-outer polygons for Σ in this case, we should therefore pick a subsequence of levels. For example, pick T_{2k} and H_{2k} for $k \in \mathbb{N}$. Once again (G1), (G2), and (G4) will be satisfied for $0 < \delta < \frac{1}{2}$, but now

$$\mathrm{dist}(\partial\Sigma_{2k}, \partial[(\Sigma_{2k+2})_{\delta\ell_{2k+2}}]) \leq \frac{\ell_{2k}}{5} + \frac{\delta\ell_{2k+2}}{\frac{\sqrt{2}}{2}} = \frac{\ell_{2k}}{5} + \frac{\delta\ell_{2k}\sqrt{2}}{5}.$$

And (G3) is guaranteed for

$$\mathrm{dist}(\partial\Sigma_{2k}, \partial[(\Sigma_{2k+2})_{\delta\ell_{2k+2}}]) < \delta\ell_{2k},$$

which implies $\delta > \frac{1}{5-\sqrt{2}}$ with the right hand side of this less than $1/2$. Hence all four conditions of the Hypothesis G hold whenever we pick only the even levels for $\frac{1}{5-\sqrt{2}} \approx 0.2789 < \delta < 1/2$; see Figure 4 (right).

From Lemma 2.6 we get $\omega_1^2(\mathsf{T}_{2k}) - \omega_1^2(\mathsf{H}_{2k}) \to 0$ as $k \to \infty$ at a rate at least $\frac{1}{5^{\frac{k}{2}}}$.

3. Conformal transplantation

We now turn to block W2). Let $f \equiv f_j \colon \Omega_0 \to \Omega_j$ be the conformal map of Ω_0 to the corresponding level Ω_j. Here we consider Ω_j as subsets of the complex plane. When instead the polygons are viewed as lying in the two-dimensional real plane $\mathbb{R}^2$, the coordinates are denoted by $y = (y_1, y_2) \in \Omega_0$ and $x = (x_1, x_2) \in \Omega_j$. We also denote by $f \colon \mathbb{R}^2 \to \mathbb{R}^2$ the map given in real coordinates:

$$y \longmapsto x = f(y) = (f^1(y), f^2(y)).$$

The following standard manipulations involving the composition map associated with f will be useful in later sections. As f is analytic, it satisfies the Cauchy-Riemann equations:

$$\partial_1 f^1 = \partial_2 f^2 \quad \text{and} \quad \partial_2 f^1 = -\partial_1 f^2.$$

Hence

$$\nabla_y f = \begin{bmatrix} \partial_1 f^1 & -\partial_2 f^1 \\ \partial_2 f^1 & \partial_1 f^1 \end{bmatrix},$$

$$\det(\nabla_y f) = |f'|^2, \quad \text{and} \quad (\nabla_y f)(\nabla_y f)^T = |f'|^2 \begin{bmatrix} 1 & 0 \\ 0 & 1 \end{bmatrix},$$

where

$$|f'|^2 = (\partial_1 f^1)^2 + (\partial_2 f^1)^2 = (\partial_1 f^2)^2 + (\partial_2 f^2)^2.$$

Let $u \in C^2(\Omega_j)$ and $v = u \circ f$. Then

$$\operatorname{grad}_y v = \nabla_y (u \circ f) = (\nabla_y f)^T \nabla_x u \circ f$$

and

$$\begin{aligned}
\Delta_y v &= \operatorname{div}_y \operatorname{grad}_y v \\
&= \nabla_y \cdot [(\nabla_y f)^T \nabla_x u \circ f] \\
&= [\nabla_x u \circ f] \cdot \Delta f + \operatorname{Tr}[(\nabla_y f)^T (D_x^2 u \circ f)(\nabla_y f)] \\
&= 0 + \operatorname{Tr}[(\nabla_y f)^T (D_x^2 u \circ f)(\nabla_y f)] \\
&= |f'|^2 \Delta_x u \circ f.
\end{aligned}$$

Here $D_x^2 u$ denotes the Hessian

$$D_x^2 u = \begin{bmatrix} \partial_{11}^2 u & \partial_{12}^2 u \\ \partial_{21}^2 u & \partial_{22}^2 u \end{bmatrix}$$

and $\underline{\Delta} f$ the vector Laplacian

$$\underline{\Delta} f = \begin{bmatrix} \Delta f^1 \\ \Delta f^2 \end{bmatrix}.$$

Also

$$\int\limits_{\Omega_0} |v(y)|^2 |f'(y)|^2 dy = \int\limits_{\Omega_j} |u(x)|^2 dx < \infty \tag{11}$$

and

$$\int\limits_{\Omega_0} |\nabla_y v(y)|^2 dy = \int\limits_{\Omega_j} |\nabla_x u(x)|^2 dy < \infty, \tag{12}$$

whenever $u \in H^1(\Omega_j)$.

The above calculations indicate that if u is an eigenfunction of (2) for $\Omega = \Omega_j$, then $v = u \circ f$ solves the transplanted eigenvalue problem

$$\begin{aligned} -\Delta v &= \omega^2 |f'|^2 v \quad \text{in } \Omega_0, \\ v &= 0 \qquad\qquad \text{on } \partial\Omega_0. \end{aligned} \tag{13}$$

Moreover, if v is an eigenfunction of (13), then $u = v \circ f^{-1}$ is an eigenfunction of (2) associated with the same eigenvalue. As we shall see later in Theorem 4.2 there is a one-to-one correspondence between the eigenfunctions of the Dirichlet Laplacian on Ω_j and those of a selfadjoint operator associated to (13). This is neither obvious nor an immediate consequence of classical principles, as $|f'|$ has zeros and poles on the boundary of the domain.

There are two reasons for preferring (13) over (2). One is that, even though both u and v have singularities, v is more regular than u. The other reason is related to the fact that our polygons will have thousands of vertices. With techniques developed in [2, 3] we are able to efficiently and accurately compute the conformal map f, even in these extreme situations. Solving the eigenvalue problem on Ω_0, especially for the ground eigenvalue, requires much simpler and smaller meshes than we would have needed on domains Ω_j with a highly complex boundary. This approach was also used in [1] to compute eigenvalues of fractal regions.

3.1. The Schwarz–Christoffel maps for the Koch Snowflake. In this subsection we assume that Σ is a Koch snowflake. We also consider Ω_0 as a subset of the complex plane with the variable denoted by z and Ω_j subset of the complex plane with the variable denoted by w. Denote by w_k the corners of the polygon Ω_j and by z_k their pre-images under the map f, so that $f(z_k) = w_k$. In the case

of the polygons T_0 and T_j, we order the vertices so that $w_k = z_k$ for $k = 1, 2, 3$. That is, the first three vertices of T_j are the vertices of the original triangle T_0. Similarly, for polygons H_0 and H_j we require that $w_k = z_k$ for $k = 1, \ldots, 6$. The ordering of the remaining vertices is not important.

Remark 3.1. A conformal map between two domains is not unique, but can be made so by fixing three boundary points. For T_j this immediately ensures uniqueness. For H_j, due to symmetries, we are able to fix six vertices.

We denote the interior angles of Ω_j by $\pi \alpha_k$.

- If $\Omega_j = T_j$, $\alpha_k = 1/3$ for $k = 1, 2, 3$ and $\alpha_k = 1/3$ or $4/3$ for $k > 3$. The total number of corners of T_j is

$$n(j) = 4^j 3 = \underbrace{3 + (4^j - 1)}_{\alpha_k = 1/3} + \underbrace{2(4^j - 1)}_{\alpha_k = 4/3}.$$

- If $\Omega_j = H_j$, $\alpha_k = 2/3$ for $k = 1, \ldots, 6$ and $\alpha_k = 2/3$ or $5/3$ for $k > 6$. The total number of corners of H_j is

$$n(j) = 4^j 6 = \underbrace{6 + 4(4^j - 1)}_{\alpha_k = 2/3} + \underbrace{2(4^j - 1)}_{\alpha_k = 5/3}.$$

We construct the conformal map f_j in two steps by means of an intermediate mapping onto $D = \{|z| < 1\}$. Set

$$f(z) \equiv f_j(z) = g_j \circ g_0^{-1}(z), \tag{14}$$

where the conformal map $g_j : D \to \Omega_j$ is given by the Schwarz–Christoffel formula

$$g_j(\xi) = A_j + C_j \int^{\xi} \prod_{k=1}^{n(j)} (1 - \zeta/\xi_k)^{\alpha_k - 1} d\zeta,$$

where we left out the lower integration limit as it only influences the constant A_j. The position of ξ_k, each on the unit circle ∂D, is initially unknown and needs to be computed by solving a non-linear system of equations [16]. Due to the symmetries, we can fix the first three/six pre-vertices, the pre-vertices that map to the three/six corners of the triangle/hexagon, all to be equally spaced points on ∂D. In other words, $g_j(\xi_k) = w_k = z_k$, $k = 1, \ldots, m$. Here and elsewhere $m = 3$ for T_j and $m = 6$ for H_j. For all k we have the following relationships

$$z_k = g_0(\xi_k), \quad f_j(z_k) = g_j(\xi_k) = w_k.$$

Note that

$$f'_j(z) = \frac{1}{g'_0(g_0^{-1}(z))} g'_j(g_0^{-1}(z)) = \frac{C_j}{C_0} \prod_{k=m+1}^{n(j)} (1 - g_0^{-1}(z)/\xi_k)^{\alpha_k - 1}$$

$$= \frac{C_j}{C_0} \prod_{k=m+1}^{n(j)} (1 - g_0^{-1}(z)/g_0^{-1}(z_k))^{\alpha_k - 1}. \tag{15}$$

As expected, the singularities near the $m = 3$ or $m = 6$ fixed corners have disappeared. Integrating the above formula we obtain a Schwarz–Christoffel formula for f

$$f_j(z) = \tilde{A}_j + \frac{C_j}{C_0} \int^z \prod_{k=m+1}^{n(j)} (1 - g_0^{-1}(\zeta)/g_0^{-1}(z_k))^{\alpha_k - 1} d\zeta. \tag{16}$$

The following result on the regularity of f is a consequence of this formula.

Proposition 3.2. *Let $f(z)\colon \Omega_0 \to \Omega_j$ be the conformal map defined by* (16)*. Then, f is analytic in a neighbourhood of $z_1, \ldots, z_m$. Moreover*

$$f(z) = w_k + (z - z_k)^{\alpha_k} \tilde{f}_k(z) \quad \text{for all } k > m$$

where $\tilde{f}_k(z)$ is analytic in a neighbourhood of z_k and $\tilde{f}_k(z_k) \neq 0$.

3.2. Schwarz–Christoffel map for general fractals.

In the general case we still choose f as the conformal map from Ω_0 to Ω_j, but the choice of prevertices would depend on the geometry and symmetries of the fractal. Using the same arguments as in (15), we have that

$$f(z) = w_k + (z - z_k)^{\alpha_k - \beta_k + 1} \tilde{f}_k(z)$$

with $\tilde{f}_k(z)$ a function analytic and non-zero in the neighbourhood of the prevertex z_k, $\alpha_k \pi$ the interior angle of Ω_j at corner w_k and $\beta_k \pi$ the interior angle of Ω_0 at z_k. If z_k is not a corner, $\beta_k = 1$ and we obtain the same behaviour as described in Proposition 3.2 for the Koch snowflake.

In the subsequent analysis we will need to determine the behaviour of $|f'(z)|^{-1}$ near the prevertices. From the above, it follows that

$$|f'(z)|^{-1} \sim |z - z_k|^{\beta_k - \alpha_k} \quad \text{as } z \to z_k.$$

In particular for $|f'(z)|^{-2}$ to be integrable in two dimensions, a condition we will require in the analysis, we need $\alpha_k - \beta_k < 1$. Note that this condition holds

always if $\beta_k = 1$ as $\alpha_k \in (0, 2)$. So, as long as we choose the conformal map in such a way that it sends corners of Ω_0 to corners of Ω_j with $\alpha_k - \beta_k < 1$, the above is integrable. We formulate this as an assumption, which holds for the Koch snowflake construction described above.

Assumption B. The conformal map $f: \Omega_0 \to \Omega_j$ is such that for each vertex z_k of Ω_0 mapped to a vertex w_k of Ω_j, we have $\alpha_k - \beta_k < 1$. Here $\alpha_k \pi$ is the interior angle of Ω_j at w_k, and $\beta_k \pi$ is the interior angle of Ω_0 at z_k. Note that this implies that

$$\int_{\Omega_0} |f'(z)|^{-2} dz < \infty.$$

For the Koch snowflake we fix the conformal map so that $\beta_k = \alpha_k$.

3.3. Singularities of the eigenmodes. Let $u: \Omega_j \to \mathbb{R}$ be an eigenfunction of (2) associated with an eigenvalue ω^2 for $\Omega = \Omega_j$.

Proposition 3.3. *Let (r, θ) be the local polar coordinates of $x \in \Omega_j$ with the origin at the vertex w_k. Let $R > 0$ be such that $R < \min_{i \neq k} \mathrm{dist}(w_k, w_i)$ and $R < \frac{\pi}{2|\omega|}$. Then for $r \in (0, R)$*

$$u(x) = \sum_{n=1}^{\infty} a_n J_{\frac{n}{\alpha_k}}(|\omega| r) \sin\left(\frac{n\theta}{\alpha_k}\right),$$

where

$$a_n = \frac{2}{\alpha_k \pi J_{\frac{n}{\alpha_k}}(|\omega| R)} \int_0^{\alpha_k \pi} u(R, \theta) \sin\left(\frac{n\theta}{\alpha_k}\right) d\theta, \quad n \in \mathbb{N}.$$

Proof. The proof is obtained in the usual way by separation of variables. $\qquad \square$

Remark 3.4. The condition $R < \frac{\pi}{2|\omega|}$ ensures that $J_{\frac{n}{\alpha_k}}(|\omega| R)$ is non-zero. Further, we have

$$\left| a_n J_{\frac{n}{\alpha_k}}(|\omega| r) \right| \leq C \left(\frac{r}{R}\right)^{\frac{n}{\alpha_k}},$$

giving absolute convergence of the series; see [11].

Now, let $v = u \circ f: \Omega_0 \to \mathbb{R}$ be the transplanted eigenfunction for the eigenvalue ω^2 of (13), where $f: \Omega_0 \to \Omega_j$ is the Schwarz–Christoffel map (16) in the case of the Koch snowflake.

Proposition 3.5 (Koch snowflake). *Let (ϱ, φ) be the local polar coordinates of $y \in \Omega_0$ with the origin at the pre-vertex z_k. Then*

(1) *For $\Omega_j = \mathsf{T}_j$*

$$v(y) = b_k(\varphi)\varrho^3 + O(\varrho^5), \quad for \ k = 1, 2, 3,$$
$$v(y) = b_k(\varphi)\varrho + O(\varrho^{5/3}), \quad for \ k > 3 \ and \ \alpha_k = 1/3,$$
$$v(y) = b_k(\varphi)\varrho + O(\varrho^2), \quad for \ k > 3 \ and \ \alpha_k = 4/3.$$

(2) *and for $\Omega_j = \mathsf{H}_j$*

$$v(y) = b_k(\varphi)\varrho^{3/2} + O(\varrho^3), \quad for \ k = 1, \dots, 6,$$
$$v(y) = b_k(\varphi)\varrho + O(\varrho^2), \quad for \ k > 6 \ and \ \alpha_k = 2/3,$$
$$v(y) = b_k(\varphi)\varrho + O(\varrho^2), \quad for \ k > 6 \ and \ \alpha_k = 5/3.$$

In the above, $b_k(\varphi)$ are analytic functions of φ for $\varrho e^{i\varphi} \in \Omega_0$. These functions are different for each corner.

Proof. Recall the Maclaurin expansion of Bessel functions for $\nu > 0$ [29, 10.2.2],

$$J_\nu(z) = \left(\frac{1}{2}z\right)^\nu \sum_{\ell=0}^\infty (-1)^\ell \frac{\left(\frac{1}{4}z^2\right)^\ell}{\ell!\Gamma(\nu + \ell + 1)}. \tag{17}$$

If $k \leq m$, note that the singularity at z_k of v is the same as that of u, since f is analytic near z_k and $f(z_k) = z_k$. The result is then obtained from Proposition 3.3 and the fact that ν is integer.

Next we give the details for $k > m$. Combining Proposition 3.2 and Proposition 3.3, it follows that

$$v(y) = v(z) = \sum_{n=1}^\infty a_n J_{\frac{n}{\alpha_k}}(|\omega|r) \sin\left(\frac{n\theta}{\alpha_k}\right)$$

near z_k, where

$$re^{i\theta} = \varrho^{\alpha_k} e^{i\alpha_k\varphi} \tilde{f}_k(z)$$

and the analytic function $\tilde{f}_k(z)$ is as in Proposition 3.2. In order to make use of the expansion (17), consider the terms of the form

$$r^{n/\alpha_k + 2\ell} = \varrho^{n + 2\ell\alpha_k} |\tilde{f}_k(z)|^{n/\alpha_k + 2\ell} \quad n = 1, 2, \dots \text{ and } \ell = 0, 1, \dots.$$

Note that $|\tilde{f}_k(z)|^{n/\alpha_k + 2\ell}$ is an analytic function of ϱ and φ in the vicinity of z_k since $\tilde{f}_k(z_k) \neq 0$. Further

$$\theta = \alpha_k\varphi + \operatorname{Arg} \tilde{f}_k(z).$$

The result is obtained by isolating the leading term in each one of the cases. $\quad\square$

Two remarks are now in place.

As a consequence of this proposition, in the case of the Koch snowflake, it follows that the strongest singularity for T_j is near the angles $\alpha_k = 1/3$ and for H_j near the 6 original corners. Therefore, overall, the transplantation has reduced the strongest singularity from $r^{3/4}$ to $\varrho^{5/3}$ for T_j and from $r^{3/5}$ to $\varrho^{3/2}$ for H_j. This implies, for example, that the first derivative of v is bounded but the first derivative of u is unbounded.

In the case of the T_j polygons, the original eigenfunction u is analytic near the three vertices w_k, $k = 1, 2, 3$, and the same holds for the transplanted eigenfunction near the corresponding prevertices z_k.

4. Formulation as a system

In this section we set the theoretical framework of the block W3). For this purpose we define a selfadjoint operator $\overline{\mathcal{T}_y}$ of order 1 associated with the eigenvalue problem (13), whose squared non-zero spectrum coincides with the eigenvalues of (2). In Section 5 we will formulate a procedure for computing lower and upper bounds for $\mathrm{spec}(\overline{\mathcal{T}_y})$, which involves the square of this operator. For this, the trial functions are required to lie in the operator domain of $\overline{\mathcal{T}_y}$ (the domain of the quadratic form associated to $\overline{\mathcal{T}_y}^2$). In Section 4.2 we describe explicitly an operator core $\mathcal{D}$ in terms of the derivative of the conformal map $|f'|$.

4.1. The div-grad operator. Let

$$
\overbrace{\begin{bmatrix} 0 & i\,\mathrm{div}_x \\ i\,\mathrm{grad}_x & 0 \end{bmatrix}}^{\mathcal{G}_x} : \overbrace{\begin{matrix} H_0^1(\Omega_j) \\ \times \\ H(\mathrm{div}, \Omega_j) \end{matrix}}^{\mathrm{D}(\mathcal{G}_x)} \longrightarrow \overbrace{\begin{matrix} L^2(\Omega_j) \\ \times \\ L^2(\Omega_j)^2 \end{matrix}}^{L^2(\Omega_j)^3} .
$$

The densely defined operator $\mathcal{G}_x : \mathrm{D}(\mathcal{G}_x) \to L^2(\Omega_j)^3$ is selfadjoint, because the adjoint of the minimal operator $i\,\mathrm{grad}_x : H_0^1(\Omega_j) \to L^2(\Omega_j)^2$ is the maximal operator $i\,\mathrm{div}_x : H(\mathrm{div}, \Omega_j) \to L^2(\Omega_j)$ and vice versa. Note that all the Hilbert spaces considered in this paper are on the field of complex values.

Denote the selfadjoint operator associated to (2) on $\Omega = \Omega_j$ by

$$
-\Delta_x : \mathrm{D}(\Delta_x) \longrightarrow L^2(\Omega_j).
$$

Here the domain of the Dirichlet Laplacian is defined via von Neumann's theorem [21, p. 275], as

$$
\mathrm{D}(\Delta_x) = \{u \in H_0^1(\Omega_j) : \mathrm{grad}\, u \in H(\mathrm{div}, \Omega_j)\} \subset L^2(\Omega_j).
$$

See Appendix A.

Lemma 4.1. *The non-zero vector $\left[\begin{smallmatrix} u \\ \underline{s} \end{smallmatrix}\right] \in D(\mathcal{G}_x)$ is an eigenfunction of $\mathcal{G}_x$ if and only if,*

(1) *either $u \in D(\Delta_x)$, $-\Delta_x u = \omega^2 u$ and $\underline{s} = \frac{\pm i}{|\omega|} \operatorname{grad}_x u$*

(2) *or $u = 0$ and $\operatorname{div}_x \underline{s} = 0$.*

Moreover, $\left[\begin{smallmatrix} u \\ \underline{s} \end{smallmatrix}\right]$ is associated to the eigenvalue $\pm\omega$ in the case 1 and to the eigenvalue 0 in the case 2.

Proof. See Lemma A.1 and the proof of Lemma A.2. □

Denote by $\{u_k\}_{k\in\mathbb{N}} \subset D(\Delta_x)$ an orthonormal basis of eigenfunctions such that $-\Delta_x u_k = \omega_k^2 u_k$. If $\underline{s}_k = \frac{\pm i}{|\omega_k|} \operatorname{grad}_x u_k$ and $\{\underline{\sigma}_n\}_{n=1}^{\infty} \subset H(\operatorname{div}, \Omega_j)$ is an orthonormal basis of $\ker(\operatorname{div})$ then, as a consequence of Lemma 4.1, the family

$$\mathcal{E} = \left\{ \begin{bmatrix} u_k \\ \pm \underline{s}_k \end{bmatrix} \right\}_{k\in\mathbb{N}} \cup \left\{ \begin{bmatrix} 0 \\ \underline{\sigma}_n \end{bmatrix} \right\}_{n\in\mathbb{N}}$$

is a complete family of eigenfunctions of $\mathcal{G}_x$. Moreover

$$\operatorname{spec}(\mathcal{G}_x) = \{\pm\omega_k(\Omega_j), 0\}.$$

In fact $\mathcal{E}$ is an orthonormal basis of $L^2(\Omega_j)^3$. Each non-zero eigenvalue is discrete and the eigenvalue zero is degenerate (infinite multiplicity).

4.2. The transplanted selfadjoint operator. Let

$$\mathcal{D} := \left\{ \begin{bmatrix} \tilde{v} \\ \underline{t} \end{bmatrix} \in L^2(\Omega_0)^3 \colon |f'|^{-1}\tilde{v} \in H_0^1(\Omega_0), \, |f'|^{-1}\operatorname{div}_y \underline{t} \in L^2(\Omega_0) \right\}$$

and define

$$\mathcal{T}_y = \begin{bmatrix} 0 & i|f'|^{-1}\operatorname{div}_y \\ i \operatorname{grad}_y |f'|^{-1} & 0 \end{bmatrix} \colon \mathcal{D} \longrightarrow L^2(\Omega_0)^3.$$

Then $\mathcal{T}_y$ is a densely defined symmetric operator.

Theorem 4.2. *The operator $(\mathcal{T}_y, \mathcal{D})$ on $L^2(\Omega_0)^3$ has an orthonormal basis of eigenfunctions in its domain. The closure*

$$\overline{\mathcal{T}_y} \colon D(\overline{\mathcal{T}_y}) \longrightarrow L^2(\Omega_0)^3$$

is selfadjoint. Moreover,

$$\operatorname{spec}(\overline{\mathcal{T}_y}) = \operatorname{spec}(\mathcal{G}_x) = \{\pm w_k(\Omega_j), 0\}.$$

The rest of this section is devoted to the proof of this theorem. Our first task will be to verify that the transplanted eigenfunctions are in the domain of $\mathfrak{T}_y$. Let

$$v_k = u_k \circ f, \qquad\qquad \tilde{v}_k = |f'|v_k,$$
$$\underline{t}_k = (\nabla_y f)^T \underline{s}_k \circ f, \quad \underline{\tau}_n = (\nabla_y f)^T \underline{\sigma}_n \circ f.$$

Lemma 4.3. *We have*

$$\widetilde{\mathcal{E}} = \left\{ \begin{bmatrix} \tilde{v}_k \\ \pm\underline{t}_k \end{bmatrix}, \begin{bmatrix} 0 \\ \underline{\tau}_n \end{bmatrix} \right\}_{k,n\in\mathbb{N}} \subset \mathcal{D}.$$

Proof. Let us first show that

$$\begin{bmatrix} \tilde{v}_k \\ \pm\underline{t}_k \end{bmatrix} \in \mathcal{D}.$$

From (12) with $u = u_k$ and $v = v_k$, it follows that

$$\int_{\Omega_0} |\nabla_y v_k|^2 dy < \infty.$$

Since Ω_0 is compact, by Sobolev embedding it then follows that also

$$\int_{\Omega_0} |v_k|^2 dy < \infty$$

and $|f'|^{-1}\tilde{v}_k = v_k \in H_0^1(\Omega_0)$. This is the first condition in the definition of $\mathcal{D}$.
   Now the second condition. Since

$$\int_{\Omega_0} |\underline{t}_k|^2 dy = \int_{\Omega_0} [(\nabla_y f)(\nabla_y f)^T (\underline{s}_k \circ f)] \cdot (\underline{s}_k \circ f) dy = \int_{\Omega_j} |\underline{s}_k|^2 dx$$

we gather that $\underline{t}_k \in L^2(\Omega_0)^2$. Then

$$\begin{aligned}
\operatorname{div}_y \underline{t}_k &= (\underline{s}_k \circ f) \cdot \underline{\Delta} f + \operatorname{Tr}\left((\nabla_y f)^T \nabla_y (\underline{s}_k \circ f)\right) \\
&= 0 + \operatorname{Tr}\left((\nabla_y f)^T [(\nabla_y \underline{s}_k)^T \circ f](\nabla_y f)\right) \\
&= |f'|^2 \operatorname{div}_x \underline{s}_k \circ f.
\end{aligned}$$

Hence

$$|f'|^{-1} \operatorname{div}_y \underline{t}_k = |f'| \operatorname{div}_x \underline{s}_k \circ f,$$

so

$$\int_{\Omega_0} ||f'|^{-1} \operatorname{div}_y \underline{t}_k|^2 dy = \int_{\Omega_0} |f'|^2 |\operatorname{div}_x \underline{s}_k \circ f|^2 dy = \int_{\Omega_j} |\operatorname{div}_x \underline{s}_k|^2 dx < \infty.$$

This is the second condition in the definition of $\mathcal{D}$.

It is only left to show that

$$\begin{bmatrix} 0 \\ \pm \underline{\tau}_n \end{bmatrix} \in \mathcal{D}.$$

On the one hand,

$$\int_{\Omega_0} |\underline{\tau}_n|^2 dy = \int_{\Omega_0} [(\nabla_y f)(\nabla_y f)^T (\underline{\sigma}_n \circ f)] \cdot (\underline{\sigma}_n \circ f) dy = \int_{\Omega_j} |\underline{\sigma}_n|^2 dx.$$

On the other hand,

$$\text{div}_y \, \underline{\tau}_n = |f'|^2 \, \text{div}_x \, \underline{\sigma}_n \circ f = 0 \in L^2(\Omega_0). \qquad \square$$

The family $\widetilde{\mathcal{E}}$ in this lemma is a family of eigenfunctions of $\mathcal{T}_y$. Indeed

$$\begin{aligned}
\mathcal{T}_y \begin{bmatrix} \tilde{v}_k \\ \pm \underline{t}_k \end{bmatrix} &= \begin{bmatrix} \pm i |f'|^{-1} \, \text{div}_y \, \underline{t}_k \\ i \, \text{grad}_y \, v_k \end{bmatrix} \\
&= \begin{bmatrix} \pm i |f'| (\text{div}_x \, \underline{s}_k) \circ f \\ i (\nabla_y f)^T (\text{grad}_x \, u_k) \circ f \end{bmatrix} \\
&= \begin{bmatrix} |f'| & 0 \\ 0 & (\nabla_y f)^T \end{bmatrix} \mathcal{G}_x \begin{bmatrix} u_k \\ \pm \underline{s}_k \end{bmatrix} \circ f \\
&= \pm \omega_k \begin{bmatrix} |f'| u_k \circ f \\ \pm (\nabla_y f)^T \underline{s}_k \circ f \end{bmatrix} \\
&= \pm \omega_k \begin{bmatrix} \tilde{v}_k \\ \pm \underline{t}_k \end{bmatrix}
\end{aligned}$$

and

$$\mathcal{T}_y \begin{bmatrix} 0 \\ \underline{\tau}_n \end{bmatrix} = \begin{bmatrix} i |f'| (\text{div}_x \, \underline{\sigma}_n) \circ f \\ 0 \end{bmatrix} = 0.$$

In fact it is a complete family of eigenfunctions as we shall see next.

Lemma 4.4.

$$\text{Span} \, \widetilde{\mathcal{E}} = L^2(\Omega_0)^3.$$

Proof. We verify that $\widetilde{\mathcal{E}}^\perp = \{0\}$. Suppose that

$$\int_{\Omega_0} \begin{bmatrix} \tilde{v}_k \\ \pm \underline{s}_k \end{bmatrix} \cdot \begin{bmatrix} v \\ \underline{t} \end{bmatrix} dy = 0 = \int_{\Omega_0} \begin{bmatrix} 0 \\ \underline{\tau}_n \end{bmatrix} \cdot \begin{bmatrix} v \\ \underline{t} \end{bmatrix} dy \quad \text{for all } k, n \in \mathbb{N}. \qquad (18)$$

Let $g = f^{-1} \colon \mathbb{R}^2 \to \mathbb{R}^2$ be the inverse map to f. Then $u = v \circ g$ and $\underline{s} = \underline{t} \circ g$ and

$$
\begin{aligned}
0 &= \int_{\Omega_0} \begin{bmatrix} |f'| u_k \circ f \\ \pm (\nabla_y f)^T \underline{s}_k \circ f \end{bmatrix} \cdot \begin{bmatrix} u \circ f \\ \underline{s} \circ f \end{bmatrix} dy \\
&= \int_{\Omega_0} \begin{bmatrix} u_k \circ f \\ \pm \underline{s}_k \circ f \end{bmatrix} \cdot \begin{bmatrix} |f'| u \circ f \\ (\nabla_y f) \underline{s} \circ f \end{bmatrix} dy \\
&= \int_{\Omega_j} \begin{bmatrix} u_k \\ \pm \underline{s}_k \end{bmatrix} \cdot \begin{bmatrix} |g'| u \\ |g'|^2 ((\nabla_y f) \circ g) \underline{s} \end{bmatrix} dx
\end{aligned}
$$

for all $k \in \mathbb{N}$. Further

$$
0 = \int_{\Omega_j} |g'|^2 \underline{\sigma}_n \cdot (\nabla_y f \circ g) \underline{s} \; dx
$$

for all $n \in \mathbb{N}$. Since $\mathcal{E}$ is an orthonormal basis of $L^2(\Omega_j)^3$, then

$$
|g'| u = 0 \quad \text{and} \quad |g'|^2 (\nabla_y f \circ g) \underline{s} = 0.
$$

Hence, since $|g'| \neq 0$ a.e. and $\det \nabla_y f \circ g = |g'|^{-2} \neq 0$ a.e., $u = 0$ and $\underline{s} = 0$. Thus (18) implies $\begin{bmatrix} v \\ \underline{t} \end{bmatrix} = 0$. $\qquad\square$

In order to generate an orthonormal family of eigenfunctions apply Gram-Schmidt to $\widetilde{\mathcal{E}}$ which might not be orthonormal a priori. Note that in fact $\mathcal{T}_y$ is essentially selfadjoint, [13, Lemma 1.2.2]. This completes the proof of Theorem 4.2.

Remark 4.5. Since $|f'|$ has singularities on $\partial \Omega_0$, it is not a priori clear whether $(\mathcal{T}_y, \mathcal{D})$ is closed. This is a rather subtle point. We are unaware of any investigation in this respect.

5. Computation of upper and lower bounds

We now describe one possible method to determine bounds for the eigenvalues of the operator $\overline{\mathcal{T}_y}$ for the block W4). We have chosen the quadratic method [24] which fully avoids spectral pollution [32] and is shown to be reliable for computing eigenvalues. For a full list of references see [6, Section 6.1]. For alternative approaches see [27, 34, 9, 20, 5].

5.1. The quadratic method. Given a subspace $\mathcal{L} \subset \mathrm{D}(\overline{\mathcal{T}_y})$ of dimension $d < \infty$, the second order spectrum [14] of $\overline{\mathcal{T}_y}$ relative to $\mathcal{L}$ is the spectrum of the following quadratic matrix polynomial weak eigenvalue problem.

Problem 5.1. Find $\lambda \in \mathbb{C}$ and $0 \neq \begin{bmatrix} v \\ t \end{bmatrix} \in \mathcal{L}$ such that

$$\left\langle (\overline{\mathcal{T}_y} - \lambda) \begin{bmatrix} v \\ t \end{bmatrix}, (\overline{\mathcal{T}_y} - \lambda^*) \begin{bmatrix} \tilde{v} \\ \tilde{t} \end{bmatrix} \right\rangle = 0 \quad \text{for all } \begin{bmatrix} \tilde{v} \\ \tilde{t} \end{bmatrix} \in \mathcal{L}.$$

Given a basis for the subspace $\mathcal{L}$,

$$\mathcal{L} = \mathrm{span}\{\underline{b}_j\}_{j=1}^d,$$

and writing

$$\begin{bmatrix} v \\ t \end{bmatrix} = \sum_{j=1}^d \alpha_j \underline{b}_j \quad \text{for } \underline{\alpha} = (\alpha_j)_{j=1}^d \in \mathbb{C}^d,$$

this problem becomes equivalent to

$$Q(\lambda)\underline{\alpha} = 0 \quad \text{for } Q(z) = K - 2zL + z^2 M,$$

where

$$K = [\langle \overline{\mathcal{T}_y} \underline{b}_j, \overline{\mathcal{T}_y} \underline{b}_k \rangle]_{j,k=1}^d, \quad L = [\langle \overline{\mathcal{T}_y} \underline{b}_j, \underline{b}_k \rangle]_{j,k=1}^d, \quad M = [\langle \underline{b}_j, \underline{b}_k \rangle]_{j,k=1}^d.$$

The $\lambda \in \mathbb{C}$ solutions to Problem 5.1 are therefore the spectrum of the quadratic matrix polynomial $Q(z)$. Since $Q(z)$ is selfadjoint, this set is symmetric with respect to the real line. Since $\det M \neq 0$, it consists of at most $2d$ distinct isolated points.

The following relation between the second order spectra and the spectrum of $\overline{\mathcal{T}_y}$ is crucial below. Let

$$\mathbb{D}(a,b) = \left\{ z \in \mathbb{C} \colon \left| z - \frac{a+b}{2} \right| < \frac{b-a}{2} \right\}.$$

Then,

$$\left. \begin{array}{l} (a,b) \cap \mathrm{spec}\, \overline{\mathcal{T}_y} = \{\omega\} \\ \det Q(\lambda) = 0 \\ \lambda \in \mathbb{D}(a,b) \end{array} \right\} \implies \mathrm{Re}\,\lambda - \frac{|\mathrm{Im}\,\lambda|^2}{b - \mathrm{Re}\,\lambda} < \omega < \mathrm{Re}\,\lambda + \frac{|\mathrm{Im}\,\lambda|^2}{\mathrm{Re}\,\lambda - a}. \quad (19)$$

See [33, Remark 2.3] and [8, Corollary 2.6].

5.2. Finite element approximation of the eigenvalue bounds. We now show a possible concrete family of subspaces $\mathcal{L}$. Let Ξ_h be a uniform triangulation of Ω_0, define the corresponding space of piecewise polynomials to be

$$\widehat{\mathcal{L}} = \left\{ \begin{bmatrix} v \\ \underline{t} \end{bmatrix} \in C^0(\overline{\Omega_0})^3 \colon \begin{bmatrix} v|_K \\ \underline{t}|_K \end{bmatrix} \in \mathbb{P}_p(K)^3 \text{ for all } K \in \Xi_h, \, v|_{\partial\Omega_0} = 0 \right\}, \quad (20)$$

and let

$$F = \begin{bmatrix} |f'| & 0 & 0 \\ 0 & 1 & 0 \\ 0 & 0 & 1 \end{bmatrix}.$$

Consider the following reformulation of Problem 5.1.

Problem 5.2. Find λ and $0 \neq \begin{bmatrix} v \\ \underline{t} \end{bmatrix} \in \widehat{\mathcal{L}}$ such that for all $\begin{bmatrix} \tilde{v} \\ \tilde{\underline{t}} \end{bmatrix} \in \widehat{\mathcal{L}}$

$$\left\langle F^{-1}\mathcal{G}_y \begin{bmatrix} v \\ \underline{t} \end{bmatrix}, F^{-1}\mathcal{G}_y \begin{bmatrix} \tilde{v} \\ \tilde{\underline{t}} \end{bmatrix} \right\rangle - 2\lambda \left\langle \mathcal{G}_y \begin{bmatrix} v \\ \underline{t} \end{bmatrix}, \begin{bmatrix} \tilde{v} \\ \tilde{\underline{t}} \end{bmatrix} \right\rangle + \lambda^2 \left\langle F \begin{bmatrix} v \\ \underline{t} \end{bmatrix}, F \begin{bmatrix} \tilde{v} \\ \tilde{\underline{t}} \end{bmatrix} \right\rangle = 0.$$

The substitution $\begin{bmatrix} v \\ \underline{t} \end{bmatrix} = F^{-1}\begin{bmatrix} w \\ \underline{r} \end{bmatrix}$ and $\begin{bmatrix} \tilde{v} \\ \tilde{\underline{t}} \end{bmatrix} = F^{-1}\begin{bmatrix} \tilde{w} \\ \tilde{\underline{r}} \end{bmatrix}$ yields an equivalence between problems 5.2 and 5.1, where the subspaces are deformed by the action of $|f'|$,

$$\mathcal{L} = F\widehat{\mathcal{L}}. \quad (21)$$

Indeed Problem 5.2 is equivalent to finding λ and $0 \neq \begin{bmatrix} w \\ \underline{r} \end{bmatrix} \in \mathcal{L}$ such that

$$\left\langle \overline{\mathcal{T}_y} \begin{bmatrix} w \\ \underline{r} \end{bmatrix}, \overline{\mathcal{T}_y} \begin{bmatrix} \tilde{w} \\ \tilde{\underline{r}} \end{bmatrix} \right\rangle - 2\lambda \left\langle \overline{\mathcal{T}_y} \begin{bmatrix} w \\ \underline{r} \end{bmatrix}, \begin{bmatrix} \tilde{w} \\ \tilde{\underline{r}} \end{bmatrix} \right\rangle + \lambda^2 \left\langle \begin{bmatrix} w \\ \underline{r} \end{bmatrix}, \begin{bmatrix} \tilde{w} \\ \tilde{\underline{r}} \end{bmatrix} \right\rangle = 0 \quad \text{for all } \begin{bmatrix} \tilde{w} \\ \tilde{\underline{r}} \end{bmatrix} \in \mathcal{L}.$$

The latter is exactly Problem 5.1 for $\mathcal{L}$ given by (21). For the quadratic method to be free from spectral pollution we require $\mathcal{L} \subset D(\overline{\mathcal{T}_y})$. As we shall see next, this is indeed the case.

Lemma 5.3. *Let $\widehat{\mathcal{L}}$ be given by (20) and $\mathcal{L}$ be given by (21). Then $\mathcal{L} \subset \mathcal{D}$.*

Proof. Let $\begin{bmatrix} \tilde{v} \\ \tilde{\underline{t}} \end{bmatrix} \in \widehat{\mathcal{L}}$. Since $\widehat{\mathcal{L}} \subset H_0^1(\Omega_0) \times H^1(\Omega_0)^2$, then $\tilde{v} \in H_0^1(\Omega_0)$ and $\underline{t} \in H^1(\Omega_0)^2 \subset H(\text{div}, \Omega_0)$. As the first entry of $F\begin{bmatrix} \tilde{v} \\ \tilde{\underline{t}} \end{bmatrix}$ is $|f'|\tilde{v}$, it indeed satisfies the first condition in the definition of $\mathcal{D}$.

Now, the second entry of $F\begin{bmatrix} \tilde{v} \\ \tilde{\underline{t}} \end{bmatrix}$ is $\underline{t}$. Since $\underline{t}$ is continuous and piecewise polynomial its divergence is bounded on $\overline{\Omega_0}$. Hence

$$\int_{\Omega_0} ||f'|^{-1} \text{div}_y \, \underline{t}|^2 dy \leq \| \text{div}_y \, \underline{t} \|_\infty^2 \int_{\Omega_0} |f'|^{-2} dy.$$

The function $|f'|^{-1}$ has singularities only on $\partial\Omega_0$. According to Assumption B,

$$\int_{\Omega_0} |f'|^{-2} dy < \infty.$$

Then, indeed $|f'|^{-1} \operatorname{div}_y \underline{t} \in L^2(\Omega_0)$, ensuring the second condition in the definition of $\mathcal{D}$. $\qquad\square$

Remark 5.4. Let

$$\begin{bmatrix} \tilde{v}_1 \\ \underline{t}_1 \end{bmatrix} \in \widetilde{\mathcal{E}}$$

be the normalised eigenfunction associated to the first positive eigenvalue

$$\omega_1(\Omega_j) \in \operatorname{spec}(\overline{\mathcal{T}_y}).$$

A convergence analysis of the finite element method at individual Ω_j can be carried out in the context of [7, Theorem 3.2]. It shows that if there exists a constant $c_1 > 0$ so that

$$\inf_{[w_h\ \underline{r}_h]^T \in \mathcal{L}} \left\| \begin{bmatrix} \tilde{v}_1 \\ \underline{t}_1 \end{bmatrix} - \begin{bmatrix} w_h \\ \underline{r}_h \end{bmatrix} \right\|_{L^2(\Omega_0)^3} + \left\| \mathcal{T}_y\left(\begin{bmatrix} \tilde{v}_1 \\ \underline{t}_1 \end{bmatrix} - \begin{bmatrix} w_h \\ \underline{r}_h \end{bmatrix} \right) \right\|_{L^2(\Omega_0)^3} < c_1 h^p,$$

then there exists λ_h such that $\det Q(\lambda_h) = 0$ and

$$|\lambda_h - \omega_1| < c_2 h^{p/2}.$$

The hypothesis translates into the subspace $\hat{\mathcal{L}}$ as follows:

$$\inf_{[v_h\ \underline{r}_h]^T \in \hat{\mathcal{L}}} \left\| \begin{bmatrix} |f'|v_1 \\ \underline{t}_1 \end{bmatrix} - \begin{bmatrix} |f'|v_h \\ \underline{r}_h \end{bmatrix} \right\|_{L^2(\Omega_0)^3}$$
$$+ \left\| F^{-1}\mathcal{G}_y\left(\begin{bmatrix} |f'|v_1 \\ \underline{t}_1 \end{bmatrix} - \begin{bmatrix} |f'|v_h \\ \underline{r}_h \end{bmatrix} \right) \right\|_{L^2(\Omega_0)^3} < c_1 h^p.$$

Here $v_1 = u_1 \circ f$. These convergence estimates might be investigated in future work.

6. Computations for a Koch snowflake

In this section we show a particular implementation of the workflow W1)–W4) for the Koch snowflake Σ inscribed in the unit disk D. This implementation leads to (1). In [12, Table 2] an approximation of the ground eigenvalue for the hexagon

Table 1. For level $j = 10$. Upper and lower bounds for the ground eigenvalue on H_{10} and T_{10}. The mesh is made of equilateral triangles. At each refinement we increase the number of triangles by a factor of 4.

$\omega_1^2(H_{10})^{\text{upper}}_{\text{lower}}$	Refinement
13.1^{17}_{04}	2
13.11^{61}_{49}	3
13.11^{61}_{57}	4
13.11^{61}_{59}	5
13.1160^{16}_{02}	6
13.11601^{20}_{15}	7

$\omega_1^2(T_{10})^{\text{upper}}_{\text{lower}}$	Refinement
$13.\cdot^{12}_{09}$	4
13.1^{17}_{03}	5
13.11^{65}_{26}	6
13.11^{63}_{57}	7
13.116^{24}_{16}	8
13.1162^{29}_{08}	9
13.11622^{76}_{10}	10

was reported as $\omega_1^2(H_0) \leq 7.155339146$. Later in [1, Table 2] numerical evidence was given indicating that $\omega_1^2(\Sigma) = 13.116184\bar{3}$ with doubt over the last digit. This number is within the estimate (1).

In block W1) we set $j = 1, \ldots, 10$ where T_j and H_j are chosen as in Section 2.1. We find upper and lower bounds for $\omega_1^2(T_j)$ and $\omega_1^2(H_j)$. By domain monotonicity (3) lower bounds for $\omega_1^2(H_j)$ are lower bounds for $\omega_1^2(\Sigma)$ and upper bounds for $\omega_1^2(T_j)$ are upper bounds for $\omega_1^2(\Sigma)$. We derive (1) from

$$\omega_1^2(H_{10})_{\text{lower}} < \omega_1^2(\Sigma) < \omega_1^2(T_{10})^{\text{upper}}$$

using the numerical estimates in the last row of Table 1.

We compute the conformal maps f_j for block W2) by means of the highly accurate procedure described in [3, 2] coded in C++. The Schwarz–Christoffel formula (16) is semi-explicit as the position of the pre-vertices z_k for $j > 0$ is not a-priori known and needs to be computed as the solution of a non-linear parameter problem. Using a simple iteration due to Davis [15] and accelerating the computation using the fast multipole method [18], we solve this problem for hundreds of thousands of pre-vertices. The details and required modifications to the original algorithms are given in [2, 3].

For block W4), we solve Problem 5.2. We pick Lagrange elements of order $p = 5$ in (20) on a mesh for Ω_0 made of uniformly distributed equilateral triangles of identical area. We start with an initial mesh for H_0 made of 6 equilateral triangles and T_0 made of 4 equilateral triangles. Then refine each mesh a number of times. In each refinement the number of elements is multiplied by 4.

The ground eigenvalue on the unit disk is $\omega_1^2(D) = j_{0,1}$ and $14.68 < j_{1,1} = \omega_2^2(D)$. To get lower bounds for $\omega_1(\Omega_j)$, we appeal to (3) and consider (19) fixing

$a = 0$ and $b \leq \omega_2(\mathsf{D})$. In practice we choose

$$b < \sqrt{j_{1,1}}.$$

We formulated and solved Problem 5.2 numerically using the commercial package Comsol Multiphysics and ran the simulations in Comsol Livelink for Matlab.

6.1. Our best estimate. In Table 1 we show our computation of $\omega_1^2(\mathsf{T}_{10})$ and $\omega_1^2(\mathsf{H}_{10})$, as we refine the original mesh the indicated number of times.

For T_{10} accuracy stalls from the 6th to the 7th refinement, then it jumps by a considerable margin. We believe that this phenomenon is linked to the structure of the eigenfunction for T_{10} near the boundary, but we can say no more at present. Similarly a stall in accuracy occurs between the 3rd and 5th refinement for H_{10}.

We stopped the calculation due to lack of computer memory for T_{10} after 10 refinements and for H_{10} after 7 refinements.

6.2. The optimal rate of interior-exterior domain approximation. In order to test optimality of the decreasing rate of

$$\omega_1^2(\mathsf{T}_j) - \omega_1^2(\mathsf{H}_j)$$

established in Lemma 2.2, we present in Table 2 computation of $\omega_1^2(\Omega_j)$ with the shown number of refinements for $j = 0, \ldots, 10$. Note that

$$\omega_1^2(\mathsf{T}_0) = \frac{16\pi^2}{9} \leq 17.54597.$$

Therefore the lower bound for level $j = 0$ is not given, because the b chosen in (19) is not below $\omega_1(\mathsf{T}_0)$.

Let the mean of the computed bounds at corresponding level for region Ω_j be

$$\tilde{\omega}_1^2(\Omega_j) = \frac{\omega_1^2(\Omega_j)^{\text{upper}} + \omega_1^2(\Omega_j)_{\text{lower}}}{2}.$$

On the right of Table 2 we show a semilog (vertical axis) plot of

$$r(j) = \tilde{\omega}_1^2(\mathsf{T}_j) - \tilde{\omega}_1^2(\mathsf{H}_j)$$

versus $j = 2, \ldots, 10$. Remarkably, the picture shows a near straight line, suggesting that, to high accuracy, the law
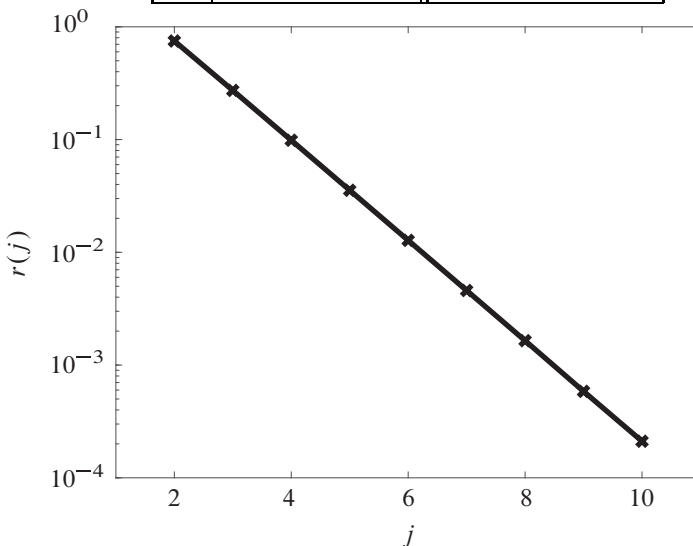
$$r(j) \approx C\rho^j$$

is satisfied. Our computed values give $\rho \approx 0.35958$ and

$$C \approx 5.8688.$$

See the Remark 2.3. In [1] this observation was used to accelerate by extrapolation the convergence to the eigenvalues of the fractal.

Table 2. For level $j = 0, \ldots, 10$. Top. Upper and lower bounds for the ground eigenvalue on H_j and T_j. The refinement used in each case is as shown in the columns R. Bottom. Semilog plot of $r(j)$.

j	$\omega_1^2(\mathsf{H}_j)^{\text{upper}}_{\text{lower}}$	R	$\omega_1^2(\mathsf{T}_j)^{\text{upper}}_{\text{lower}}$	R
0	7.15533^{94}_{83}	4	17.5459633^{80}	4
1	11.78144^{39}_{19}	5	13.402^{73}_{24}	5
2	12.51986^{87}_{72}	6	13.268^{86}_{56}	6
3	12.89778^{23}_{06}	7	13.170^{77}_{69}	7
4	13.03710^{92}_{57}	7	13.1357^{54}_{33}	8
5	13.0876^{93}_{89}	7	13.123^{22}_{19}	8
6	13.10593^{82}_{52}	7	13.118^{71}_{68}	8
7	13.112^{51}_{49}	7	13.1170^{93}_{73}	8
8	13.1148^{63}_{59}	7	13.116^{52}_{49}	8
9	13.11570^{99}_{73}	7	13.116^{31}_{28}	9
10	13.11601^{20}_{15}	7	13.11622^{76}_{10}	10

Appendix A. Spectrum of the matrix operator

The results presented in this appendix are common knowledge. However, as we could not find a suitable reference to the specific statement that we required in Section 3, we include full details of proofs.

Let $\mathfrak{H}_1$ and $\mathfrak{H}_2$ be two possibly different separable Hilbert spaces. Let $T : D(T) \to \mathfrak{H}_2$ be a densely defined closed operator from $D(T) \subset \mathfrak{H}_1$ and let

$$\mathcal{E} = \begin{bmatrix} 0 & T^* \\ T & 0 \end{bmatrix}.$$

The operator

$$\mathcal{E} : D(T) \oplus D(T^*) \longrightarrow \mathfrak{H}_1 \oplus \mathfrak{H}_2$$

is selfadjoint, indeed note that $(T^*)^* = \bar{T} = T$. Moreover, by von Neumann's Theorem [21, p. 275], we know that both $T T^* : D(T T^*) \to \mathfrak{H}_1$ and $T^* T : D(T^* T) \to \mathfrak{H}_2$ are selfadjoint in the corresponding domains of operator multiplication (of closed operators). Also $D(T^* T) \subset \mathfrak{H}_1$ is a core for T and $D(T T^*) \subset \mathfrak{H}_1$ is a core for T^*. As we shall see next, the spectrum of $\mathcal{E}$ is fully characterised by the spectra of $T T^*$ and $T^* T$. Below, the point spectrum is denoted by spec_p.

Lemma A.1. $0 \in \mathrm{spec}_\mathrm{p}(\mathcal{E})$ *if and only if* $0 \in \mathrm{spec}_\mathrm{p}(T T^*) \cup \mathrm{spec}_\mathrm{p}(T^* T)$. *Moreover*

$$\dim \mathrm{Ker}(\mathcal{E}) = \dim \mathrm{Ker}(T^* T) + \dim \mathrm{Ker}(T T^*).$$

Proof. Since

$$\mathcal{E} \begin{bmatrix} u \\ v \end{bmatrix} = 0 \iff T^* v = 0 \text{ and } Tu = 0$$
$$\iff T T^* v = 0 \text{ and } T^* T u = 0,$$

the first claim follows.

For the second claim note that there is a one-to-one correspondence between a set of eigenvectors $\{ \begin{bmatrix} u_n \\ \pm v_n \end{bmatrix} \}$ associated to $0 \in \mathrm{spec}_\mathrm{p}(\mathcal{E})$ and $\{ \begin{bmatrix} u_n \\ 0 \end{bmatrix}, \begin{bmatrix} 0 \\ v_n \end{bmatrix} \}$, which possibly has some zero vectors. $\qquad\square$

In the above statement zero can be in the point spectrum of one of the operators $T T^*$ or $T^* T$ but not necessarily the other. This is for example the case for T the standard shift in $\ell^2(\mathbb{N})$.

Lemma A.2. *Let $\lambda \neq 0$. The following are equivalent*:

- $\lambda \in \mathrm{spec}_p(\mathcal{E})$;
- $-\lambda \in \mathrm{spec}_p(\mathcal{E})$;
- $\lambda^2 \in \mathrm{spec}_p(TT^*)$;
- $\lambda^2 \in \mathrm{spec}_p(T^*T)$.

Moreover

$$
\dim \mathrm{Ker}(\mathcal{E} - \lambda) = \dim \mathrm{Ker}(\mathcal{E} + \lambda)
$$
$$
= \dim \mathrm{Ker}(T^*T - \lambda^2)
$$
$$
= \dim \mathrm{Ker}(TT^* - \lambda^2).
$$

Proof. Let $\lambda \in \mathrm{spec}_p(\mathcal{E})$ and $\dim \mathrm{Ker}(\mathcal{E} - \lambda) = m$. Then there exists a linearly independent set

$$
\left\{ \begin{bmatrix} u_n \\ v_n \end{bmatrix} \right\}_{n=1}^{m} \subset \mathrm{D}(\mathcal{E})
$$

such that

$$
(\mathcal{E} - \lambda) \begin{bmatrix} u_n \\ v_n \end{bmatrix} = 0.
$$

Then $T^*v_n = \lambda u_n$ and $Tu_n = \lambda v_n$ and, necessarily, $u_n \neq 0$ and $v_n \neq 0$ for all $n \in \{1, \ldots, m\}$. Thus also the set $\left\{ \begin{bmatrix} u_n \\ -v_n \end{bmatrix} \right\}_{n=1}^{m}$ is linearly independent and $(\mathcal{E} + \lambda) \begin{bmatrix} u_n \\ -v_n \end{bmatrix} = 0$. Therefore $-\lambda \in \mathrm{spec}_p(\mathcal{E})$ and $\dim \mathrm{Ker}(\mathcal{E} + \lambda) = m$.

Now, as

$$
\left\{ \begin{bmatrix} \frac{1}{\lambda} T^* v_n \\ v_n \end{bmatrix} \right\}_{n=1}^{m} = \left\{ \begin{bmatrix} u_n \\ v_n \end{bmatrix} \right\}_{n=1}^{m},
$$

the former is a linearly independent set of eigenvectors with $v_n \in \mathrm{D}(T^*)$ and $T^*v_n \in \mathrm{D}(T)$. Then $TT^*v_n = \lambda^2 v_n$ for the set of non-zero vectors $\{v_n\}_{n=1}^{m} \subset \mathrm{D}(TT^*)$. Assume that $\dim \mathrm{Ker}(TT^* - \lambda^2) = l < m$. Then

$$
\{v_n\}_{n=1}^{m} \subset \mathrm{span}\{\tilde{v}_j\}_{j=1}^{l}
$$

for a linearly independent set $\{\tilde{v}_j\}_{j=1}^{l}$. Hence

$$
v_k = \sum_{j=1}^{l} a_j \tilde{v}_j \quad \text{and} \quad T^*v_k = \sum_{j=1}^{l} a_j T^* \tilde{v}_j
$$

for some $k \in \{1, \ldots, m\}$. Thus

$$
\begin{bmatrix} \frac{1}{\lambda} T^* v_k \\ v_k \end{bmatrix} = \sum_{j=1}^{l} a_j \begin{bmatrix} \frac{1}{\lambda} T^* \tilde{v}_j \\ \tilde{v}_j \end{bmatrix}
$$

which is a contradiction. Therefore $l \geq m$. But let $\tilde{u}_j = \frac{1}{\lambda} T^* \tilde{v}_j$ and consider the set $\left\{ \begin{bmatrix} \tilde{u}_j \\ \tilde{v}_j \end{bmatrix} \right\}_{j=1}^{l} \subset D(\mathcal{E})$. This is a linearly independent set of eigenvectors of $\mathcal{E}$ for λ. This shows that necessarily $l = m$.

All the above, and a symmetric argument involving u_n instead of v_n and T^*T instead of TT^*, are enough to prove the claim. $\qquad \square$

References

[1] L. Banjai, Eigenfrequencies of fractal drums. *J. Comput. Appl. Math.* **198** (2007), no. 1, 1–18. MR 2250385 Zbl 1103.65111

[2] L. Banjai, Revisiting the crowding phenomenon in Schwarz–Christoffel mapping. *SIAM J. Sci. Comput.* **30** (2008), no. 2, 618–636. MR 2385878 Zbl 1165.30004

[3] L. Banjai and L. N. Trefethen, A multipole method for Schwarz–Christoffel mapping of polygons with thousands of sides. *SIAM J. Sci. Comput.* **25** (2003), no. 3, 1042–1065. MR 2046124 Zbl 1060.30012

[4] G. Barrenechea, L. Boulton, and N. Boussaïd, Finite element eigenvalue enclosures for the Maxwell operator. *SIAM J. Sci. Comput.* **36** (2014), no. 6, A2887–A2906. MR 3285902 Zbl 1317.78012

[5] G. Barrenechea, L. Boulton, and N. Boussaïd, Local two-sided bounds for eigenvalues of self-adjoint operators. *Numer. Math.* **135** (2017), no. 4, 953–986. MR 3621822 Zbl 1375.65074

[6] L. Boulton, Spectral pollution and eigenvalue bounds. *Appl. Numer. Math.* **99** (2016), 1–23. MR 3413891 Zbl 1329.65261

[7] L. Boulton and A. Hobiny, On the convergence of the quadratic method. *IMA J. Numer. Anal.* **36** (2016), no. 3, 1310–1333. MR 3523586 Zbl 1433.65266

[8] L. Boulton and M. Levitin, On approximation of the eigenvalues of perturbed periodic Schrödinger operators. *J. Phys. A* **40** (2007), no. 31, 9319–9329. MR 2345295 Zbl 1120.81033

[9] C. Carstensen and J. Gedicke, Guaranteed lower bounds for eigenvalues. *Math. Comp.* **83** (2014), no. 290, 2605–2629. MR 3246802 Zbl 1320.65162

[10] E. Cesàro, Remarques sur la courbe de von Koch. *Napoli Atti* (2) **12** (1905), no. 15, 12 pp. JFM 36.0445.02 JFM 36.0445.03

[11] S. N. Chandler-Wilde and S. Langdon, A Galerkin boundary element method for high frequency scattering by convex polygons. *SIAM J. Numer. Anal.* **45** (2007), no. 2, 610–640. MR 2300290 Zbl 1162.35020

[12] L. Cureton and J. Kuttler, Eigenvalues of the Laplacian on regular polygons and polygons resulting from their dissection. *J. Sound Vibration* **220** (1999), no. 1, 83–98. MR 1672258 Zbl 1235.35206

[13] E. B. Davies, *Spectral theory and differential operators*. Cambridge Studies in Advanced Mathematics, 42. Cambridge University Press, Cambridge, 1995. MR 1349825 Zbl 0893.47004

[14] E. B. Davies, Spectral enclosures and complex resonances for general self-adjoint operators. *LMS J. Comput. Math.* **1** (1998), 42–74. MR 1635727 Zbl 0931.47021

[15] R. T. Davis, Numerical methods for coordinate generation based on Schwarz–Christoffel transformations. In *4th Computational Fluid Dynamics Conference.* Williamsburg, VA, July 23–25, 1979. American Institute of Aeronautics and Astronautics, Reston, VA, 1979, 1–15.

[16] T. A. Driscoll and L. N. Trefethen, *Schwarz–Christoffel mapping.* Cambridge Monographs on Applied and Computational Mathematics, 8. Cambridge University Press, Cambridge, 2002. MR 1908657 Zbl 1003.30005

[17] M. Gardner, In which "monster" curves force redefinition of the word "curve". *Sci. Amer.* **236** (1976), 124–133.

[18] L. Greengard, *The rapid evaluation of potential fields in particle systems.* ACM Distinguished Dissertations. MIT Press, Cambridge, MA, 1988. MR 0936632 Zbl 1001.31500

[19] C. A. Griffith and M. L. Lapidus, Computer graphics and the eigenfunctions for the Koch snowflake drum. In S. I. Andersson and M. L. Lapidus (eds.), *Progress in inverse spectral geometry.* Trends in Mathematics. Birkhäuser Verlag, Basel, 1997, 95–113. MR 1731153 Zbl 1044.58504

[20] X. Liu, A framework of verified eigenvalue bounds for self-adjoint differential operators. *Appl. Math. Comput.* **267** (2015), 341–355. MR 3399052 Zbl 1410.35088

[21] T. Kato, *Perturbation theory for linear operators.* Reprint of the 1980 edition. Classics in Mathematics. Springer-Verlag, Berlin, 1995. MR 1335452 Zbl 0836.47009

[22] M. L. Lapidus, J. W. Neuberger, R. J. Renka, and C. A. Griffith, Snowflake harmonics and computer graphics: numerical computation of spectra on fractal drums. *Internat. J. Bifur. Chaos Appl. Sci. Engrg.* **6** (1996), no. 7, 1185–1210. MR 1412217 Zbl 0920.73165

[23] M. L. Lapidus and M. M. H. Pang, Eigenfunctions of the Koch snowflake domain. *Comm. Math. Phys.* **172** (1995), no. 2, 359–376. MR 1350412 Zbl 0857.35093

[24] M. Levitin and E. Shargorodsky, Spectral pollution and second order relative spectra for self-adjoint operators. *IMA J. Numer. Anal.* **24** (2004), no. 3, 393–416. MR 2068829 Zbl 1060.65056

[25] B. B. Mandelbrot, *Fractals*: *form, chance, and dimension.* Translated from the French. Revised edition. W. H. Freeman and Co., San Francisco, CA, 1977. MR 0471493 Zbl 0376.28020

[26] B. B. Mandelbrot, *The fractal geometry of nature.* Schriftenreihe für den Referenten. W. H. Freeman and Co., San Francisco, CA, 1982. MR 0665254 Zbl 0504.28001

[27] M. Marletta and R. Scheichl, Eigenvalues in spectral gaps of differential operators. *J. Spectr. Theory* **2** (2012), no. 3, 293–320. MR 2947289 Zbl 1256.65079

[28] J. M. Neuberger, N. Sieben, and J. W. Swift, Computing eigenfunctions on the Koch snowflake: a new grid and symmetry. *J. Comput. Appl. Math.* **191** (2006), no. 1, 126–142. MR 2217789 Zbl 1094.35085

[29] F. W. J. Olver, D. W. Lozier, R. F. Boisvert, and C. W. Clark (eds.), *NIST handbook of mathematical functions.* U.S. Department of Commerce, National Institute of Standards and Technology, Washington, D.C., and Cambridge University Press, Cambridge, 2010. MR 2723248 Zbl 1198.00002

[30] M. M. H. Pang, Approximation of ground state eigenvalues and eigenfunctions of Dirichlet Laplacians. *Bull. London Math. Soc.* **29** (1997), no. 6, 720–730. MR 1468060 Zbl 0969.35102

[31] G. Rozenberg and A. Salomaa, *The mathematical theory of L-systems.* APure and Applied Mathematics, 90. Academic Press, New York and London, 1980. MR 0561711 Zbl 0508.68031

[32] E. Shargorodsky, Geometry of higher order relative spectra and projection methods. *J. Operator Theory* **44** (2000), no. 1, 43–62. MR 1774693 Zbl 0994.47003

[33] M. Strauss, Quadratic projection methods for approximating the spectrum of self-adjoint operators. *IMA J. Numer. Anal.* **31** (2011), no. 1, 40–60. MR 2755936 Zbl 1214.65026

[34] I. Šebestová and T. Vejchodský, Two-sided bounds for eigenvalues of differential operators with applications to Friedrichs, Poincaré, trace, and similar constants. *SIAM J. Numer. Anal.* **52** (2014), no. 1, 308–329. MR 3163245 Zbl 1287.35050

Lehel Banjai, Department of Mathematics, Maxwell Institute for Mathematical Sciences, Heriot-Watt University, Edinburgh EH14 4AS, Scotland

e-mail: l.banjai@hw.ac.uk

Lyonell Boulton, Department of Mathematics,
Maxwell Institute for Mathematical Sciences, Heriot-Watt University,
Edinburgh EH14 4AS, Scotland

Department of Mathematics, Faculty of Nuclear Sciences and Physical Engineering,
Czech Technical University in Prague, Trojanova 13, 12000 Prague 2, Czech Republic

e-mail: l.boulton@hw.ac.uk